

# ULD-FL: Federated Learning with Across Silo User-Level Differential Privacy

Fumiyuki Kato  
 Kyoto University  
 fumiyuki@db.soc.i.kyoto-u.ac.jp

Li Xiong  
 Emory University  
 lxiong@emory.edu

Shun Takagi  
 Kyoto University  
 takagi.shun.45a@st.kyoto-u.ac.jp

Yang Cao  
 Hokkaido University  
 yang@ist.hokudai.ac.jp

Masatoshi Yoshikawa  
 Osaka Seikei University  
 yoshikawa-mas@osaka-seikei.ac.jp

arXiv:2308.12210v1 [cs.LG] 23 Aug 2023

**Abstract**—Differentially Private Federated Learning (DP-FL) has garnered attention as a collaborative machine learning approach that ensures formal privacy. Most DP-FL approaches ensure DP at the record-level within each silo for cross-silo FL. However, a single user’s data may extend across multiple silos, and the desired user-level DP guarantee for such a setting remains unknown. In this study, we present ULD-FL, a novel FL framework designed to guarantee user-level DP in cross-silo FL where a single user’s data may belong to multiple silos. Our proposed algorithm directly ensures user-level DP through per-user weighted clipping, departing from group-privacy approaches. We provide a theoretical analysis of the algorithm’s privacy and utility. Additionally, we enhance the algorithm’s utility and showcase its private implementation using cryptographic building blocks. Empirical experiments on real-world datasets show substantial improvements in our methods in privacy-utility trade-offs under user-level DP compared to baseline methods. To the best of our knowledge, our work is the first FL framework that effectively provides user-level DP in the general cross-silo FL setting.

**Index Terms**—Federated Learning, Differential Privacy, User-level DP

## I. INTRODUCTION

Federated Learning (FL) [1] is a collaborative machine learning (ML) scheme in which multiple parties train a single global model without sharing training data. FL has attracted industry attention [2], [3] as concerns about the privacy of training data have become more serious, as exemplified by GDPR [4]. It should be noted that FL itself does not provide privacy protection for the trained model [5], [6], which motivates for *Differentially Private FL* (DP-FL) [7], [8], which guarantees a formal privacy for trained models based on differential privacy (DP) [9].

Although DP is the de facto standard in the field of statistical privacy protection, it has a theoretical limitation. The standard DP definition takes a single record as a unit of privacy. This can easily break down in a realistic setting where one user may provide multiple records, and can deteriorate the privacy loss bound of DP. To this end, the notion of *user-level DP* has been studied [10]–[13]. In user-level DP, instead of a single record, all records belonging to a single user are considered as a unit of privacy, which is a stricter definition than standard

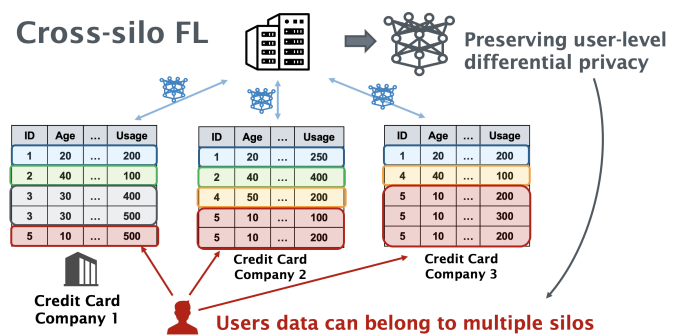


Fig. 1: In cross-silo FL, in general, records belonging to the same user can exist across silos, e.g., a user can use several credit card companies. In this study, we investigate how to train models satisfying *user-level DP* in this setting.

DP. Note that we distinguish user-level DP from *group-privacy* [14] which considers any  $k$  records as privacy units. User-level DP has also been studied in the FL context [7], [8], [15]–[17]. However, these studies focus on the cross-device FL setting, where one user’s data belongs to a single device only.

Cross-silo FL [18]–[21] is a practical variant of FL in which a relatively small number of silos (e.g., hospitals or credit card companies) participate in the training rounds. In contrast to cross-device FL, in cross-silo FL, a single user can have multiple records across silos, as shown in Figure 1. Existing cross-silo DP-FL studies [19]–[21] have focused on record-level DP for each silo; user-level DP across silos has not been studied. Therefore, our research question is: *How do we design a FL framework guaranteeing user-level DP across silos in cross-silo FL?*

A naive design for an algorithm that guarantees user-level DP is a combination of bounding user contributions (number of records) as those in [12], [13] and group-privacy property of DP [14]. Group-privacy simply extends the indistinguishability of the record-level DP to multiple records. We can convert any DP algorithm to group-privacy version of DP (Lemma 1, 5), which we formally define as Group DP (GDP) later. However, this approach can be impractical due to the super-linear privacy

bound degradation of conversion to GDP and the need to appropriately limit the maximum number of user records (group size) in a distributed environment. In particular, the former problem is a fundamental issue for DP and highlights the need to develop algorithms that directly satisfy user-level DP without requiring a conversion to GDP.

In this study, we present a novel cross-silo FL framework named ULDP-FL, designed to directly guarantee user-level DP through the incorporation of per-user weighted clipping. The contributions of our work are summarized as follows:

- We introduce a problem setting for cross-silo FL under user-level DP across silos, as illustrated in Figure 1.
- We propose the ULDP-FL framework and design baseline algorithms capable of achieving user-level DP across silos. The baseline algorithms combine limiting the maximum number of records per user and using group-privacy with DP-SGD [22] for each silo.
- Our proposed algorithm ULDP-AVG/SGD directly satisfy user-level DP by implementing user-level weighted clipping within each silo, which can effectively bound user-level sensitivity for unlimited number of a single user’s records across silos. We provide theoretical analysis on the ULDP-AVG, showing a user-level DP bound and a convergence analysis.
- We evaluate our proposed method and baseline approaches through comprehensive experiments on various real-world datasets. The results underscore that our proposed method yields superior trade-offs between privacy and utility compared to the baseline approaches.
- We further design an effective method by refining the weighting strategy for user-level clipping bounds. Since this approach may lead to additional privacy leakage of the training data, we develop a private protocol employing cryptographic techniques. We evaluate the extra computational overhead of the proposed private protocol using real-world benchmark scenarios.

## II. BACKGROUND & PRELIMINARIES

### A. Cross-silo Federated learning

In this work, we consider the following cross-silo FL scenario. We have a central aggregation server and silo set  $S$  participating in all rounds. In each round, the server aggregates models from all silos and then redistributes the aggregated models. Each silo  $s \in S$  optimizes a local model  $f_s$ , which is the expectation of a loss function  $F(x; \xi)$  that may be non-convex, where  $x \in \mathbb{R}^d$  denotes the model parameters and  $\xi$  denotes the data sample, and the expectation is taken over local data distribution  $\mathcal{D}_s$ . In cross-silo FL, we optimize this global model parameter cooperatively across all silos. Formally, the overarching goal in FL can be formulated as follows:

$$\min_x \left\{ f(x) := \frac{1}{|S|} \sum_{s \in S} f_s(x) \right\}, f_s(x) := \mathbb{E}_{\xi \sim \mathcal{D}_s} F(x; \xi). \quad (1)$$

In our work, we introduce additional notations. We have user set  $U$  across all datasets across silos, where each record

belongs to one user  $u \in U$ , and each user may have multiple records in one silo and across multiple silos. Each silo  $s$  has local objectives for each user  $u$ ,  $f_{s,u} := \mathbb{E}_{\xi \sim \mathcal{D}_{s,u}} F(x; \xi)$ , where  $\mathcal{D}_{s,u}$  is the data distribution of  $s$  and  $u$ . In round  $t \in [T]$  in FL, the global model parameter is denoted as  $x_t$ .

Note that this modeling is clearly different from cross-device FL in that there is no constraint that one user should belong to one device. Records from one user can belong to multiple silos. For example, the same customer may use several credit card companies, etc. Additionally, all silos participate in all training rounds, unlike the probabilistic participation in cross-device FL [17], and the number of silos  $|S|$  is small, around 2 to 100.

### B. Differential Privacy

DP [9] is a rigorous mathematical privacy definition that quantitatively evaluates the degree of privacy protection when publishing outputs.

**Definition 1** ( $(\epsilon, \delta)$ -DP). *A randomized mechanism  $\mathcal{M} : \mathcal{D} \rightarrow \mathcal{Z}$  satisfies  $(\epsilon, \delta)$ -DP if, for any two input databases  $D, D' \in \mathcal{D}$  s.t.  $D'$  differs from  $D$  in at most one record and any subset of outputs  $Z \subseteq \mathcal{Z}$ , it holds that*

$$\Pr[\mathcal{M}(D) \in Z] \leq \exp(\epsilon) \Pr[\mathcal{M}(D') \in Z] + \delta. \quad (2)$$

We call databases  $D$  and  $D'$  as *neighboring* databases. The maximum difference of the output for any neighboring database is referred to as *sensitivity*, as defined in Definition 4. We label the original definition as *record-level* DP because the neighboring databases differ in only one record.

To extend privacy guarantees to multiple records, group-privacy [14] has been explored as a solution. We refer to the group-privacy version of DP as Group DP (GDP) and define it as follows:

**Definition 2** ( $(k, \epsilon, \delta)$ -GDP). *A randomized mechanism  $\mathcal{M} : \mathcal{D} \rightarrow \mathcal{Z}$  satisfies  $(k, \epsilon, \delta)$ -GDP if, for any two input databases  $D, D' \in \mathcal{D}$ , s.t.  $D'$  differs from  $D$  in at most  $k$  records and any subset of outputs  $Z \subseteq \mathcal{Z}$ , Eq. (2) holds.*

GDP is a versatile privacy definition, as it can be applied to existing DP mechanisms without modification. To convert  $(\epsilon, \delta)$ -DP to  $(k, \epsilon, \delta)$ -GDP, it is known that any  $(\epsilon, 0)$ -DP mechanism satisfies  $(k, k\epsilon, 0)$ -GDP [14]. However, in the case of any  $\delta > 0$ ,  $\delta$  increases super-linearly [23], leading to a much larger  $\epsilon$  (Lemma 1). Also, we can compute GDP using group-privacy property of Rényi DP [24]. First, we calculate the RDP of the algorithm, then convert it to group version of RDP, and subsequently to GDP (Lemma 5).

Figure 2 illustrates a numerical comparison of the group-privacy conversion from DP to GDP with normal DP (Lemma 1) and RDP (Lemma 5). We repeatedly execute the Gaussian mechanism and calculate the final GDP. We plot various group sizes,  $k$ , on the x-axis and  $\epsilon$  of GDP at fixed  $\delta = 10^{-5}$  on the y-axis. The conversion of normal DP with fixed  $\delta$  is complex and elaborated in Appendix D1. Significantly, the result indicates that as the group size,  $k$ , increases,  $\epsilon$  grows

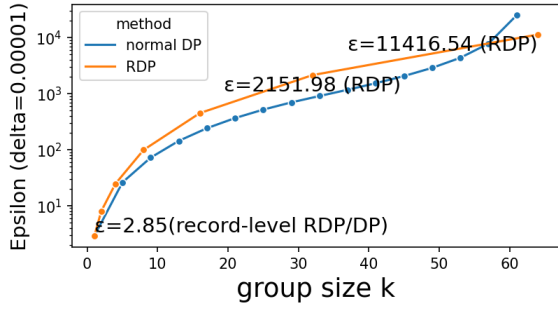


Fig. 2: Group-privacy conversion results.

rapidly, underscoring a considerable degradation in the privacy bound of GDP. For instance, with  $\epsilon = 2.85$  in record-level ( $k = 1$ ), the value reaches 2100 for only  $k = 32$ , and 11400 at  $k = 64$ . While there might be some looseness in the group-privacy conversion of RDP compared to normal DP for some small group sizes, the difference is relatively minor (roughly three times at most). And the RDP’s conversion is easier to compute with a fixed  $\delta$ . Hence, we utilize RDP’s conversion in our experiments.

### C. Differentially Private FL

DP has been applied to the FL paradigm, where the goal is to ensure that the trained model satisfies DP. A popular DP variant in the context of cross-device FL is user-level DP (also known as client-level DP) [7], [8], [25]. Informally, this definition ensures indistinguishability for device participation and has demonstrated a favorable privacy-utility trade-off even with large-scale models [17]. These studies often employ secure aggregation [26], [27] to mitigate the need for trust in other parties during FL model training. This is achieved by allowing the server and other silos to only access appropriately perturbed models after aggregation. This is often known as Distributed DP [8], [28]. In particular, *shuffling*-based variants have recently attracted a great deal of attention [28]–[30] and are being deployed in FL [31], which also provides user-level DP. All of these studies assume that a single device holds all records for a single user, i.e., cross-device FL. However, in a cross-silo setting, this definition does not extend meaningful privacy protection to individual users when they possess multiple records across silos.

Another DP definition in cross-silo FL is a variant offering record-level DP within each silo [19]–[21], which is referred to as *Silo-specific sample-level* or *Inter-silo record-level DP*. These studies suggest that record-level DP can guarantee user-level DP through group-privacy [14]. However, they cannot account for settings where a single user may have records across multiple silos. To the best of our knowledge, there exists no method for training models that satisfy user-level DP in cross-silo FL where a single user records may extend across multiple silos.

## III. ULDP-FL FRAMEWORK

### A. Trust model and Assumptions

We assume that all (two or more) silos and aggregation servers are *semi-honest*, meaning they observe the information but do not deviate from the protocol. This is a typical assumption in prior works [26], [32]. In our study, aggregation is performed using secure aggregation to ensure that the server only gains access to the model after aggregation [8]. All communications between the server and silos are encrypted with SSL/TLS, and third parties with the ability to snoop on communications cannot access any information except for the final trained model. We assume that there is no collusion, which is reasonable given that silos are socially separate institutions (such as different hospitals or companies). Additionally, in our scenario, we assume that record linkage [33] across silos has already been completed, resulting in shared common user IDs. Both the server and the silos are aware of the total number of users  $|U|$  with at least one record and the number of silos  $|S|$ .

### B. Privacy definition

In contrast to GDP, which offers indistinguishability for any  $k$  records, user-level DP [7], [11] provides a more reasonable user-level indistinguishability. While [7] focuses solely on a cross-device FL context, we re-establish user-level DP (ULDP) in the cross-silo setting as follows:

**Definition 3** ( $(\epsilon, \delta)$ -ULDP). *A randomized mechanism  $\mathcal{M} : \mathcal{D} \rightarrow \mathcal{Z}$  satisfies  $(\epsilon, \delta)$ -ULDP if, for any two input databases across silos  $D, D' \in \mathcal{D}$ , s.t.  $D'$  differs from  $D$  in at most one user’s records, and any  $Z \subseteq \mathcal{Z}$ , Eq. (2) holds.*

The fundamental difference from record-level DP lies in the definition of the neighboring databases, which inherently defines user-level sensitivity. Additionally, it is important to emphasize that the input database  $D$  represents the comprehensive database spanning across silos.

If the number of records per user in the database is less than or equal to  $k$ , it is clear that GDP is a generalization of ULDP, and the following proposition holds.

**Proposition 1.** *If a randomized mechanism  $\mathcal{M}$  is  $(k, \epsilon, \delta)$ -GDP with input database  $D$  in which any user has at most  $k$  records, the mechanism  $\mathcal{M}$  with input database  $D$  also satisfies  $(\epsilon, \delta)$ -ULDP.*

One drawback of GDP is the challenge of determining the appropriate value for  $k$ . Setting  $k$  to the maximum number of records associated with any individual user could lead to introducing excessive noise to achieve the desired privacy protection level. On the other hand, if a smaller  $k$  is chosen, the data of users with more than  $k$  records must be excluded from the dataset, potentially introducing bias and compromising model utility. In this context, while several studies have analyzed the theoretical utility for a given  $k$  [10], [11] and theoretical considerations for determining  $k$  have been partially explored in [13], it still remains an open problem. In

---

**Algorithm 1** ULDP-GROUP- $k$ 

---

**Input:**  $S$ : silo set (silo  $s \in S$ ),  $\eta_l$ : local learning rate,  $\eta_g$ : global learning rate,  $\sigma$ : noise parameter,  $D_s$ : training dataset of silo  $s$ ,  $C$ : clipping bound,  $T$ : total round,  $Q$ : #local epochs,  $k$ : group size,  $\gamma$ : sampling rate,  $\mathbf{B}$ : flags for limit contribution s.t. for each matrix  $\mathbf{b}^s \in \mathbf{B}$  if  $b_{u,i}^s = 1$  the user  $u$ 's  $i$ -th record in silo  $s$  is used in training dataset, otherwise the record is excluded

```

1: procedure SERVER
2:   Initialize model  $x_0$ 
3:   for each round  $t = 0, 1, \dots, T - 1$  do
4:     for each silo  $s \in S$  do
5:        $\Delta_t^s \leftarrow \text{CLIENT}(x_t, C, \sigma, \eta_l, \gamma, \mathbf{b}^s)$ 
6:        $\theta_{t+1} \leftarrow \theta_t + \eta_g \frac{1}{|S|} \sum_{s \in S} \Delta_t^s$ 
7:   procedure CLIENT( $x_t, C, \sigma, \eta_l, \gamma, \mathbf{b}^s$ )
8:      $D'_s \leftarrow \text{filter } D_s \text{ by } \mathbf{b}^s$ 
9:      $x_t^Q \leftarrow \text{DP-SGD}(\theta_t, D'_s, C, \sigma, \eta_l, \gamma, Q)$ 
10:    ▷ Algorithm 1 in [22]
11:     $\Delta_{t+1} \leftarrow x_t^Q - x_t$ 
12:  return  $\Delta_{t+1}$ 

```

---

contrast, ULDP does not necessitate the determination of  $k$ . Instead, it requires designing a specific ULDP algorithm.

### C. Baseline methods: ULDP-NAIVE/GROUP- $k$

We begin by describing two baseline methods. The first method is ULDP-NAIVE (described in Algorithm 3), a straightforward approach using substantial noise. It is an extension of DP-FedAVG [17], where each silo locally optimizes with multiple epochs, computing the model delta, clipping by  $C$  and adding a Gaussian noise with variance  $\sigma^2 C^2$ . In contrast, in ULDP-NAIVE, since a single user may contribute to the model delta of all silos, the sensitivity across silos is  $|C| * S$  for the aggregated model delta (Line 15). Moreover, compared to DP-FedAVG focusing on cross-device FL, the number of model delta samples (number of silos as versus number of devices) is very small, which also results in larger variance. Hence, ULDP-NAIVE satisfies ULDP at a significant sacrifice in utility. Note that any following algorithm uses secure aggregation and all of proofs of the following theorems are shown in Appendix A5.

**Theorem 1.** *For any  $0 < \delta < 1$  and  $\alpha > 1$ , given noise multiplier  $\sigma$ , ULDP-NAIVE satisfies  $(\epsilon = \frac{T\alpha}{2\sigma^2} + \log((\alpha - 1)/\alpha) - (\log \delta + \log \alpha)/(\alpha - 1), \delta)$ -ULDP after  $T$  rounds. (The actual value of  $\epsilon$  is numerically calculated by selecting the optimal  $\alpha$  so that  $\epsilon$  is minimized.)*

Secondly, we introduce the baseline algorithm ULDP-GROUP- $k$  (described in Algorithm 1), which combines the constraint of limiting each user's records to a given  $k$  while satisfying  $(k, \epsilon, \delta)$ -GDP. As proposition 1 implies, this ensures  $(\epsilon, \delta)$ -ULDP. The algorithm achieves GDP by implementing DP-SGD [22] within each silo. The algorithm's core principle is akin to that of [19], except for the global setting of a single

privacy budget across silos. Before executing DP-SGD, it is essential to constrain the number of records per user to  $k$  (Line 8). We accomplish this by employing flags, denoted as  $\mathbf{B}$ , which indicates the records to be used for training (i.e.,  $b_{u,i}^s = 1$ ), with a total of  $k$  records for each user across all silos (i.e.,  $\forall u, \sum_{s,i} b_{u,i}^s \leq k$ ). This flag must be the same for all rounds for privacy guarantee. We ignore the privacy concerns in generating the flags because this is the baseline method. Then, we perform DP-SGD to satisfy record-level DP (Line 9), which is subsequently converted to GDP.

**Theorem 2.** *For any  $0 < \delta < 1$ , any integer  $k$  to the power of 2 and  $\alpha > 2^{k+1}$ , ULDP-GROUP- $k$  satisfies  $(3^k \rho + \log((\frac{\alpha}{2^k} - 1)/\frac{\alpha}{2^k}) - (\log \delta + \log \frac{\alpha}{2^k})/(\frac{\alpha}{2^k} - 1), \delta)$ -ULDP where  $\rho = \max_{s \in S} \rho_s$  s.t. for each silo  $s \in S$ , DP-SGD of local subroutine satisfies  $(\alpha, \rho_s)$ -RDP.*

While ULDP-GROUP shares algorithmic similarities with the existing record-level DP cross-silo FL framework [19], it does present weaknesses from several perspectives: (1) It presents significant degradation of privacy bounds due to the group-privacy conversion (DP to GDP). (2) Determining the appropriate group size  $k$  is a challenging task [13]. Moreover, this process demands substantial insights into the data distribution across silos and might even breach the trust model as well as the determination of the flags  $\mathbf{B}$ . (3) Using group-privacy to guarantee ULDP requires removing records from the training dataset. This can introduce a bias and can cause a degradation in the utility [13], [34]. Our next proposed method aims to overcome these challenges.

### D. Advanced methods: ULDP-AVG/SGD

To directly satisfy ULDP without using group-privacy, we design ULDP-AVG (Algorithm 2) and ULDP-SGD (Algorithm 4). These can be seen as variants of DP-FedAVG and DP-FedSGD [17]. In most cases, DP-FedAVG is preferred in terms of privacy-utility trade-off and communication-cost while DP-FedSGD might be preferable only when we have fast networks [17], which is also the case for ULDP-AVG and ULDP-SGD. In the following analysis, we focus on ULDP-AVG.

Intuitively, ULDP-AVG limits each user's contribution to the model by training the model for each user in each silo and perform per-user per-silo clipping across all silos with globally prepared clipping weights. In each round, ULDP-AVG computes parameter deltas using a per-user dataset in each silo to achieve ULDP: selecting a user (Line 8), training local model with  $Q$  epochs using only the selected user's data (Lines 10-13), calculating model delta (Line 14) and clipping the delta (Line 15). These clipped deltas  $\Delta_t^{s,u}$  are then weighted by  $w_{s,u}$  (Line 15) and summed for all users (Line 16). As long as the weights  $w_{s,u}$  satisfies constraints  $\forall u \in U, w_{s,u} > 0$  and  $\sum_{s \in S} w_{s,u} = 1$ , each user's contribution, or *sensitivity*, to the delta aggregation  $\sum_{s \in S} \Delta_t^s$  is limited to  $C$  at most. This allows ULDP-AVG to provide user-level privacy. We will discuss better ways to determine  $\mathbf{W}$  later, but a simple way is to set  $w_{s,u} = 1/|S|$ . Compared to DP-FedAVG, ULDP-AVG increases the computational cost due to per-user local

---

**Algorithm 2** ULDP-AVG

**Input:**  $U$ : user set (user  $u \in U$ ),  $S$ : silo set (silo  $s \in S$ ),  $\eta_l$ : local learning rate,  $\eta_g$ : global learning rate,  $\sigma$ : noise parameter,  $C$ : clipping bound,  $T$ : total round,  $Q$ : #local epochs,  $\mathbf{W} = (\mathbf{w}_1, \dots, \mathbf{w}_{|S|})$ : matrix with weight for user  $u$  and silo  $s$ , and  $\forall u \in U$ ,  $w_{s,u} \in \mathbf{w}_s$  and  $\sum_{s \in S} w_{s,u} = 1$

- 1: **procedure** SERVER
- 2:   Initialize model  $x_0$
- 3:   **for** each round  $t = 0, 1, \dots, T - 1$  **do**
- 4:     **for** each silo  $s \in S$  **do**
- 5:        $\Delta_t^s \leftarrow \text{CLIENT}(x_t, \mathbf{w}_s, C, \sigma, \eta_l)$
- 6:        $x_{t+1} \leftarrow x_t + \eta_g \frac{1}{|U||S|} \sum_{s \in S} \Delta_t^s$
- 7:   **procedure** CLIENT( $x_t, \mathbf{w}_s, C, \sigma, \eta_l$ )
- 8:     **for** user  $u \in U$  **do**    $\triangleright$  per-user training with  $\mathcal{D}_{s,u}$
- 9:        $x_t^{s,u} \leftarrow x_t$
- 10:      **for** epoch  $q = 0, 1, \dots, Q - 1$  **do**
- 11:        Compute stochastic gradients  $g_{t,q}^{s,u}$
- 12:         $\triangleright \mathbb{E}[g_{t,q}^{s,u}] = \nabla f_{s,u}(x_t^{s,u})$
- 13:         $x_t^{s,u} \leftarrow x_t^{s,u} - \eta_l g_{t,q}^{s,u}$
- 14:         $\Delta_t^{s,u} \leftarrow x_t^{s,u} - x_t$
- 15:         $\tilde{\Delta}_t^{s,u} \leftarrow w_{s,u} \cdot \Delta_t^{s,u} \cdot \min\left(1, \frac{C}{\|\Delta_t^{s,u}\|_2}\right)$   $\triangleright$  per-user weighted clipping
- 16:         $\Delta_t^s \leftarrow \sum_{u \in U} \tilde{\Delta}_t^{s,u} + \mathcal{N}(0, I\sigma^2 C^2 / |S|)$
- 17:     **return**  $\Delta_t^s$

---

training iteration but keeping communication costs the same, which is likely acceptable in the cross-silo FL setting.

**Theorem 3.** For any  $0 < \delta < 1$  and  $\alpha > 1$ , given noise multiplier  $\sigma$ , ULDP-AVG satisfies  $(\epsilon = \frac{T\alpha}{2\sigma^2} + \log((\alpha - 1)/\alpha) - (\log \delta + \log \alpha)/(\alpha - 1), \delta)$ -ULDP after  $T$  rounds.

**Remark 1.** For further privacy amplification, we introduce user-level sub-sampling, which can make RDP smaller according to sub-sampled amplification theorem [35]. User-level sub-sampling must be done globally across silos. The sub-sampling can be implemented in the central server by controlling the weight  $\mathbf{W}$  for each round, i.e., all of users not sub-sampled are set to 0. This may violate privacy against the server but does not affect the DP when the final model is provided externally as discussed in C.3 of [25]. We have the detailed algorithm and experimental results to show the effectiveness of user-level sub-sampling in Appendix D4.

**Theorem 4** (Convergence analysis on ULDP-AVG). For ULDP-AVG, with assumptions 1, 2 and 3 and  $\min_x f(x) \geq f^*$ , let local / global learning rates  $\eta_l / \eta_g$  be chosen as s.t.  $\eta_g \eta_l \leq \frac{1}{3QL\bar{\alpha}_t}$  and  $\eta_l < \frac{1}{\sqrt{30QL}}$ , we have,

$$\begin{aligned}
& \frac{1}{T} \sum_{t=0}^{T-1} \mathbb{E} \left[ \|\nabla f(x_t)\|^2 \right] \\
& \leq \frac{1}{cT\eta_g\eta_l Q|S|} \left( \mathbb{E} \left[ \frac{f(x_0)}{C} \right] - \mathbb{E} \left[ \frac{f^*}{C} \right] \right) \\
& \quad + \frac{5}{2c} L^2 Q \eta_l^2 (\sigma_l^2 + 6Q\sigma_g^2) + \frac{3\bar{C}L\eta_g\eta_l\sigma_l^2}{2c|S|^2|U|} + \frac{L\eta_g\sigma^2 C^2 d}{2c\bar{C}\eta_l Q|S||U|^2} \\
& \quad + A_1 \sum_{t=0}^{T-1} \mathbb{E} \left[ \sum_{s \in S} \sum_{u \in U} (|\alpha_t^{s,u} - \tilde{\alpha}_t^{s,u}| + |\tilde{\alpha}_t^{s,u} - \bar{\alpha}_t|) \right] \\
& \quad + A_2 \sum_{t=0}^{T-1} \mathbb{E} \left[ \sum_{s \in S} \sum_{u \in U} (|\alpha_t^{s,u} - \tilde{\alpha}_t^{s,u}|^2 + |\tilde{\alpha}_t^{s,u} - \bar{\alpha}_t|^2) \right] \tag{3}
\end{aligned}$$

where  $c > 0$ ,  $\bar{C} := \max_{s,u,t} \left( \frac{C}{\max(C, \eta_l \mathbb{E}[\sum_{q \in [Q]} g_{t,q}^{s,u}])} \right)$ ,

$$\begin{aligned}
\underline{C} & := \min_{s,u,t} \left( \frac{C}{\max(C, \eta_l \mathbb{E}[\sum_{q \in [Q]} g_{t,q}^{s,u}])} \right), \quad \alpha_t^{s,u} := \frac{w_{s,u} C}{\max(C, \eta_l \mathbb{E}[\sum_{q \in [Q]} g_{t,q}^{s,u}])}, \\
\tilde{\alpha}_t^{s,u} & := \frac{w_{s,u} C}{\max(C, \eta_l \mathbb{E}[\sum_{q \in [Q]} g_{t,q}^{s,u}])}, \\
\bar{\alpha}_t & := \frac{1}{|S||U|} \sum_{s \in S} \sum_{u \in U} \tilde{\alpha}_t^{s,u}, \quad A_1 := \frac{G^2}{c\underline{C}|U|T} \text{ and} \\
A_2 & := \frac{3L\eta_g\eta_l Q G^2}{2c\underline{C}|U|T}.
\end{aligned}$$

**Remark 2.** The first three terms recover the standard convergence bound up to constants for FedAVG [36] when considering participants in the FL as user-silo pairs (i.e., we have  $|S||U|$  participants). The asymptotic bound is  $O(\frac{1}{\sqrt{|S||U|QT}} + \frac{1}{T})$ . Theorem 4 achieves this when we choose the global and local learning rates  $\eta_g = |S|\sqrt{|S||U|Q}$  and  $\eta_l = \frac{1}{\sqrt{TQL}}$ , respectively. This requires a learning rate  $|S|$  times larger than the usual FedAVG with  $|S||U|$  participants, which can be interpreted as coming from the constraint on the weights  $W$ . The fourth term is the convergence overhead due to Gaussian noise addition, and the last fifth and sixth terms are the overhead due to bias from the clippings. If both of the noise and the clipping bias are zero, the convergence rate is asymptotically the same as the FedAVG convergence rate.

**Remark 3.** The fourth term, which accounts for the overhead due to noise, differs slightly from DP-FedAVG. This term is inversely proportional to  $|S||U|^2$ . As highlighted in the previous remark, if the global learning rate is set as  $\eta_g = |S|\sqrt{|U|Q}$  in ULDP-AVG, this term becomes proportional to  $\sqrt{|U|}/|U|^2$ , which is consistent with the case of DP-FedAVG with  $|U|$  participants.

**Remark 4.** The fifth and sixth terms correspond to the overhead due to the clipping biases  $|\alpha_t^{s,u} - \tilde{\alpha}_t^{s,u}|$  and  $|\tilde{\alpha}_t^{s,u} - \bar{\alpha}_t|$ , respectively. The quantity  $|\alpha_t^{s,u} - \tilde{\alpha}_t^{s,u}|$  represents the local gradient variance across all users in all silos and can be made zero by full-batch gradient decent. The noteworthy term is  $|\tilde{\alpha}_t^{s,u} - \bar{\alpha}_t|$ . As discussed in the analysis of [37], this term is influenced by structures of the neural network and data heterogeneity. It roughly quantifies how much the magnitudes

of all gradients deviate from the global mean gradient. We may be able to minimize these values by selecting appropriate weights  $\mathbf{W}$ , guided by the following optimization problem:

$$\min_{\mathbf{W}} \sum_{s \in S} \sum_{u \in U} |\tilde{\alpha}_t^{s,u} - \bar{\alpha}_t|, \text{ s.t., } w_{s,u} > 0, \forall u, \sum_{s \in S} w_{s,u} = 1$$

$$\left( = \sum_{s \in S} \sum_{u \in U} \left| w_{s,u} C_{s,u} - \frac{1}{|S||U|} \sum_{s' \in S} \sum_{u' \in U} w_{s',u'} C_{s',u'} \right| \right)$$

where  $C_{s,u} := \frac{C}{\max(C, \eta_l \|\mathbb{E}[\sum_{q \in [Q]} g_{t,q}^{s,u}]\|)}$ .

However, it is hard to determine the optimal weights because we cannot predict the gradients norm in advance, which also can cause another privacy issue.

**Comparison to baselines.** Compared to ULDP-GROUP, ULDP-AVG satisfies ULDP without group-privacy, thus avoiding the large privacy bound caused from group-privacy conversion, choosing group size  $k$  and removing the records. ULDP-AVG can be used for an arbitrary number of records per user. Also, it differs from ULDP-NAIVE in the following point. Fundamentally, per-user clipping can be viewed as cross-user FL (instead of cross-silo FL), which ensures that each user contributes to only the user-specific portion of the aggregated model updates (i.e.,  $\sum_{s \in S} \tilde{\Delta}_t^{s,u}$ ) instead of entire aggregated update (i.e.,  $\sum_{s \in S} \Delta_t^s$ ), thereby reducing sensitivity (as illustrated in Figure 6). The user contributes only  $1/|U|$  of the entire aggregated model update, which is especially effective when  $|U|$  is large as in cross-silo FL (i.e.,  $|S| \ll |U|$ ). Moreover, compute model delta in user-level leads to lower Gaussian noise variances because of large  $|U|$  while it also introduces new biases.

#### E. Better weighting strategy with private protocol

Here we consider the bias described in Remark 4. In our ULDP-AVG algorithm, we have employed uniform clipping weights, i.e. for any  $s \in S$  and  $u \in U$ ,  $w_{s,u} = 1/|S|$ , as a feasible solution to the problem without privacy violation. However, for more sophisticated solution, we propose following weighting strategy. We set a weight  $w_{s,u}^{opt}$  for  $C_{s,u}$  according to the number of records, following the heuristic that a gradient computed from a large number of records yields a better estimation that is closely aligned with the average. This results in the smaller bias. That is, let  $n_{s,u}$  be the number of records for user  $u$  in silo  $s$ , we set the weight as

$$w_{s,u}^{opt} := \frac{n_{s,u}}{\sum_{s \in |S|} n_{s,u}}. \quad (4)$$

We empirically demonstrate the effectiveness of this strategy in the experiments. However, the crucial question arises: how can it be implemented without privacy violation?

For the aforementioned better weighting strategy, a central server could aggregate histograms encompassing the user population (number of records per user) within each silo’s dataset. Subsequently, the server could compute the appropriate weights for each silo and distribute these weights back to the respective silos. However, this approach raises significant privacy concerns. It leads to a privacy breach as the silo

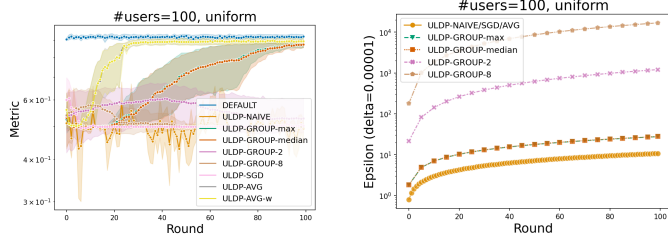
histograms are directly shared with the server. Additionally, when the server broadcasts the weights back to the silos, it enables an estimation of the entire histogram of users across all the silos, posing a similar privacy risk against other silos. In essence, the privacy protection necessitates preserving confidentiality in both of these directions. This is challenging because additive homomorphic encryption techniques such as Paillier cryptosystem cannot handle inverses to compute weights as in Eq. (4), and the raw weights are disclosed to the party with the secret key when encrypting the weights.

To address this privacy issue, we design a novel private weighting protocol to securely aggregate the user histograms from silos, compute the per-user clipping weight for each user in each silo, and aggregate the weighted sum from all silos. Our protocol leverages well-established cryptographic techniques, including secure aggregation [26], [32], the Paillier cryptosystem [38] and multiplicative blinding [39]. Intuitively, our protocol employs multiplicative blinding to hide user histograms against the server while server can compute inverses of blinded histogram to compute the weights (Eq. (4)). Subsequently, the server employs the Paillier encryption to conceal the inverses of blinded histograms because silo knows the blinded masks. Also it enables the server and silos to compute private weighted sum aggregation with its additive homomorphic property. The complete protocol and its correctness and privacy are described in Appendix B.

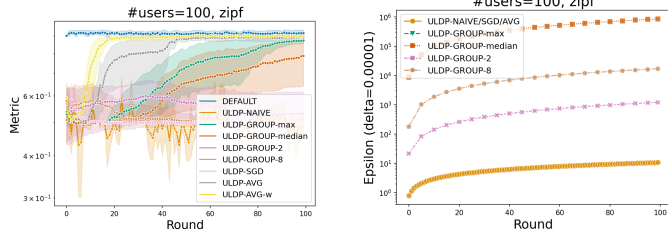
## IV. EXPERIMENTS

In this section, we evaluate the privacy-utility trade-offs of the proposed methods (ULDP-AVG/SGD), along with the previously mentioned baselines (ULDP-NAIVE/GROUP- $k$ ) and a non-private baseline (FedAVG with two-sided learning rates [36], denoted by DEFAULT). In ULDP-AVG/SGD, we set the weights as  $w_{s,u} = 1/|S|$  for all  $s$  and  $u$ , the one using  $w_{s,u}^{opt}$  is referred to as ULDP-AVG-w. Regarding ULDP-GROUP- $k$ , flags  $\mathbf{B}$  are generated for existing records to minimize waste on filtered out records, despite the potential privacy concerns. Various values, including the maximum number of user records, the median, 2, and 8, are tested as group size  $k$  and we report GDP using group-privacy conversion of RDP. In cases where  $k$  is not a power of 2, the computed  $\epsilon$  is reported for the largest power of 2 below  $k$ , showcasing the lower bound of GDP to underscore  $\epsilon$  is large. The hyperparameters, including global and local learning rates  $\eta_g, \eta_l$ , clipping bound  $C$ , and local epoch  $Q$ , are set individually for each method. Execution times are measured on macOS Monterey v12.1, Apple M1 Max Chip with 64GB memory with Python 3.9 and 3072-bit security. Most of results are averaged over 5 runs and the colored area in the graph is the standard deviation. All of implementations and experimental settings are available at <https://github.com/FumiyukiKato/uldp-fl>.

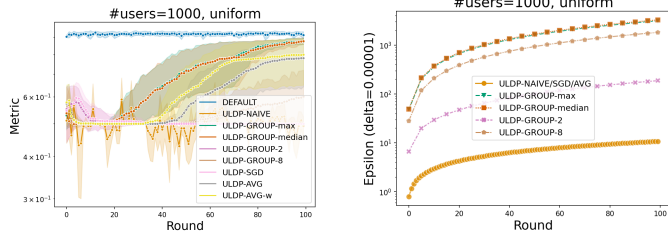
**Datasets** used in our evaluation comprise real-world open datasets, including Credicard [40] and two medical datasets, HeartDisease and TcgaBrca from [18], a benchmark datasets for cross-silo FL. We also use MNIST in Appendix. Creditcard is a popular tabular dataset for credit card fraud detection



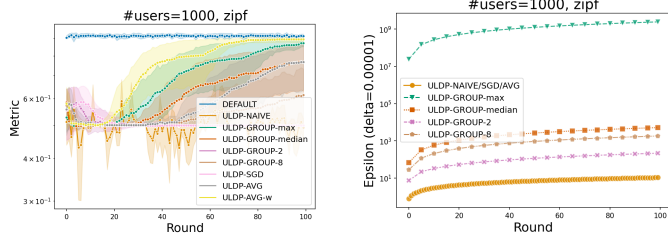
(a)  $n \approx 246$  ( $|U| = 100$ ), uniform, Test Accuracy and Privacy.



(b)  $n \approx 246$  ( $|U| = 100$ ), zipf, Test Accuracy and Privacy.



(c)  $n \approx 25$  ( $|U| = 1000$ ), uniform, Test Accuracy and Privacy.



(d)  $n \approx 25$  ( $|U| = 1000$ ), zipf, Test Accuracy and Privacy.

Fig. 3: Privacy-utility trade-offs on Creditcard dataset.

from Kaggle. We undersample the dataset and use about 25K training data and a neural network with about 4K parameters. For HeartDisease and TcgaBrca, we use the same setting such as number of silos (i.e., 4 and 6), data assignments to the silos, models, loss functions, etc. as shown in the original paper. These two datasets are quite small and the model has less than 100 parameters. For all datasets, how to allocate the records to users and silos are explained in Appendix D2.

**Privacy-utility trade-offs under ULDP.** Figures 3 show the utility and privacy evaluation results on Creditcard. The other results on MNIST, HeartDisease and TcgaBrca are shown in Appendix D4. The average number of records per user (denoting as  $n$ ) in entire silos and the distribution (uniform or zipf, as described in Appendix D2) changes for each figure. All experiments used a fixed noise parameter  $\sigma = 5.0$  and  $\delta = 10^{-5}$ , utility metrics (Accuracy for Creditcard) are

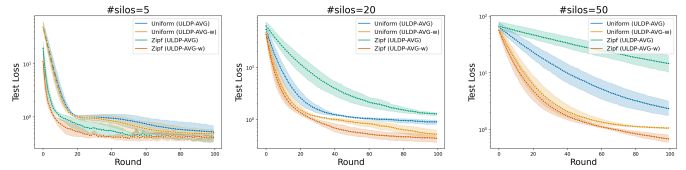


Fig. 4: Test loss of Creditcard: Weighting method is effective, especially in skewed distribution in many silos.

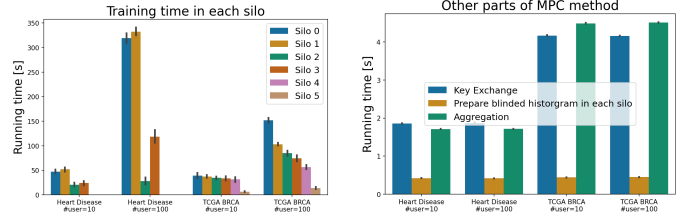


Fig. 5: With a small model, the private weighting protocol has a practical execution time.

displayed in left side and accumulated privacy consumption  $\epsilon$  for ULDP are depicted in right side. Note that the privacy bounds for ULDP-GROUP- $k$  are derived from the local DP-SGD and depend on not only the group size  $k$  but also the size of the local training dataset.

Overall, the proposed method ULDP-AVG/SGD achieves competitive utility with fast convergence and high accuracy, while achieving considerably small privacy bounds, which means the significantly better privacy-utility trade-offs compared to other baselines. We see that the baseline method, ULDP-NAIVE, has low accuracy and that ULDP-GROUP- $k$  requires much larger privacy budgets, which is consistent with the analysis on the conversion of group privacy described earlier. The convergence speed of ULDP-AVG is faster than that of ULDP-SGD, which is the same as that of DP-FedAVG/SGD. Nevertheless, there is still a gap between ULDP-AVG and the non-private method (DEFAULT) in terms of convergence speed and ultimately achievable accuracy, as a price for privacy. Also, as shown in Figure 3c, for small  $n$  (i.e., large number of users), ULDP-GROUP-max/median show higher accuracy than ULDP-AVG. This is likely due to the overhead from finer datasets at user-level, which increases the bias compared to DP-FedAVG, as seen in the theoretical convergence analysis for ULDP-AVG.

To highlight the effectiveness of the better weighting strategy, Figure 4 shows the test losses of Creditcard on different record distributions with ULDP-AVG and ULDP-AVG-w. We show the results with various number of silos 5, 20 and 50. The need for the better weight strategy is emphasized by the distribution of the records and number of silos  $|S|$ . When there is large skews in the user records, as in zipf, giving equal weights (i.e., ULDP-AVG) results in waste and opens up a large gap from ULDP-AVG-w. This trend becomes even more significant as  $|S|$  increases because all weights become smaller in ULDP-AVG.

**Overhead of private weighting protocol.** We evaluate the overheads of execution time with the private weighting protocol. Figure 5 shows the execution times following HeartDisease and TcgaBrca with the number of users 10 and 100, respectively, with a skewed (zipf) distribution. The left figure shows the time required for a local training in each silo, and the right figure shows the execution time for key exchange, preparation of blinded histograms, and aggregation. As shown in the figure, the execution time of the local training is dominant and it increases with the larger number of users. Overall, it shows realistic execution times under these benchmark scenarios [18]. However, it still causes non-negligible overhead with room for improvement in efficiency. We have more analysis with artificial dataset in Appendix D4.

## V. CONCLUSION

In this paper, we proposed the first cross-silo user-level DP FL framework where a user may have multiple records across silos and designed an algorithm using per-user clipping to directly satisfy ULDP instead of group-privacy. In addition, we developed a better weighting strategy that improves utility of our proposed method and a novel protocol that performs it privately. Finally, we demonstrated the effectiveness of the proposed method on several real-world datasets and showed that it performs significantly better than existing methods. We also verified that our proposed private protocol works in realistic time in existing cross-silo FL benchmark scenarios. Further improving the efficiency of the private protocol and the utility of ULDP algorithms to a level comparable to non-private method are future work.

## REFERENCES

- [1] H. B. McMahan, E. Moore, D. Ramage, and B. A. y Arcas, "Federated learning of deep networks using model averaging," *arXiv preprint arXiv:1602.05629*, 2016.
- [2] M. Paulik, M. Seigel, H. Mason, D. Telaar, J. Kluijvers, R. van Dalen, C. W. Lau, L. Carlson, F. Granqvist, C. Vandeveld *et al.*, "Federated evaluation and tuning for on-device personalization: System design & applications," *arXiv preprint arXiv:2102.08503*, 2021.
- [3] S. Ramaswamy, R. Mathews, K. Rao, and F. Beaufays, "Federated learning for emoji prediction in a mobile keyboard," *arXiv preprint arXiv:1906.04329*, 2019.
- [4] M. Goddard, "The eu general data protection regulation (gdpr): European regulation that has a global impact," *International Journal of Market Research*, vol. 59, no. 6, pp. 703–705, 2017.
- [5] M. Nasr, R. Shokri, and A. Houmansadr, "Comprehensive privacy analysis of deep learning: Passive and active white-box inference attacks against centralized and federated learning," in *2019 IEEE symposium on security and privacy (SP)*. IEEE, 2019, pp. 739–753.
- [6] B. Zhao, K. R. Mopuri, and H. Bilen, "idlg: Improved deep leakage from gradients," *arXiv preprint arXiv:2001.02610*, 2020.
- [7] R. C. Geyer, T. Klein, and M. Nabi, "Differentially private federated learning: A client level perspective," *NIPS 2017 Workshop: Machine Learning on the Phone and other Consumer Devices*, 2017.
- [8] P. Kairouz, Z. Liu, and T. Steinke, "The distributed discrete gaussian mechanism for federated learning with secure aggregation," in *International Conference on Machine Learning*. PMLR, 2021, pp. 5201–5212.
- [9] C. Dwork, "Differential privacy," in *Proceedings of the 33rd international conference on Automata, Languages and Programming-Volume Part II*. Springer-Verlag, 2006, pp. 1–12.
- [10] Y. Liu, A. T. Suresh, F. X. X. Yu, S. Kumar, and M. Riley, "Learning discrete distributions: user vs item-level privacy," *Advances in Neural Information Processing Systems*, vol. 33, pp. 20965–20976, 2020.
- [11] D. Levy, Z. Sun, K. Amin, S. Kale, A. Kulesza, M. Mohri, and A. T. Suresh, "Learning with user-level privacy," *Advances in Neural Information Processing Systems*, vol. 34, pp. 12466–12479, 2021.
- [12] R. J. Wilson, C. Y. Zhang, W. Lam, D. Desfontaines, D. Simmons-Marengo, and B. Gipson, "Differentially private sql with bounded user contribution," *Proceedings on privacy enhancing technologies*, vol. 2020, no. 2, pp. 230–250, 2020.
- [13] K. Amin, A. Kulesza, A. Munoz, and S. Vassilvtiskii, "Bounding user contributions: A bias-variance trade-off in differential privacy," in *International Conference on Machine Learning*. PMLR, 2019, pp. 263–271.
- [14] C. Dwork, A. Roth *et al.*, "The algorithmic foundations of differential privacy," *Foundations and Trends® in Theoretical Computer Science*, vol. 9, no. 3–4, pp. 211–407, 2014.
- [15] Ú. Erlingsson, V. Feldman, I. Mironov, A. Raghunathan, S. Song, K. Talwar, and A. Thakurta, "Encode, shuffle, analyze privacy revisited: Formalizations and empirical evaluation," *arXiv preprint arXiv:2001.03618*, 2020.
- [16] H. B. McMahan, G. Andrew, U. Erlingsson, S. Chien, I. Mironov, N. Papernot, and P. Kairouz, "A general approach to adding differential privacy to iterative training procedures," *arXiv preprint arXiv:1812.06210*, 2018.
- [17] H. B. McMahan, D. Ramage, K. Talwar, and L. Zhang, "Learning differentially private recurrent language models," *arXiv preprint arXiv:1710.06963*, 2017.
- [18] J. Ogier du Terrail, S.-S. Ayed, E. Cyffers, F. Grimberg, C. He, R. Loeb, P. Mangold, T. Marchand, O. Marfoq, E. Mushtaq, B. Muzellec, C. Philippenko, S. Silva, M. Teleńczuk, S. Albarqouni, S. Avestimehr, A. Bellet, A. Dieuleveut, M. Jaggi, S. P. Karimireddy, M. Lironzi, G. Neglia, M. Tommasi, and M. Andreux, "Flamby: Datasets and benchmarks for cross-silo federated learning in realistic healthcare settings," in *Advances in Neural Information Processing Systems*, S. Koyejo, S. Mohamed, A. Agarwal, D. Belgrave, K. Cho, and A. Oh, Eds., vol. 35. Curran Associates, Inc., 2022, pp. 5315–5334.
- [19] K. Liu, S. Hu, S. Z. Wu, and V. Smith, "On privacy and personalization in cross-silo federated learning," *Advances in Neural Information Processing Systems*, vol. 35, pp. 5925–5940, 2022.
- [20] A. Lowy and M. Razaviyayn, "Private federated learning without a trusted server: Optimal algorithms for convex losses," in *The Eleventh International Conference on Learning Representations, 2023*. [Online]. Available: <https://openreview.net/forum?id=TVY6GoURrw>
- [21] A. Lowy, A. Ghafelebashi, and M. Razaviyayn, "Private non-convex federated learning without a trusted server," in *International Conference on Artificial Intelligence and Statistics*. PMLR, 2023, pp. 5749–5786.
- [22] M. Abadi, A. Chu, I. Goodfellow, H. B. McMahan, I. Mironov, K. Talwar, and L. Zhang, "Deep learning with differential privacy," in *Proceedings of the 2016 ACM SIGSAC conference on computer and communications security*, 2016, pp. 308–318.
- [23] G. Kamath, "Cs 860 : Algorithms for private data analysis fall 2020 lecture 5 — approximate differential privacy," <http://www.gautamkamath.com/CS860notes/lec5.pdf>, 2020, [Online; accessed 23-June-2023].
- [24] I. Mironov, "Rényi differential privacy," in *2017 IEEE 30th computer security foundations symposium (CSF)*. IEEE, 2017, pp. 263–275.
- [25] N. Agarwal, P. Kairouz, and Z. Liu, "The skellam mechanism for differentially private federated learning," *Advances in Neural Information Processing Systems*, vol. 34, pp. 5052–5064, 2021.
- [26] K. Bonawitz, V. Ivanov, B. Kreuter, A. Marcedone, H. B. McMahan, S. Patel, D. Ramage, A. Segal, and K. Seth, "Practical secure aggregation for privacy-preserving machine learning," in *proceedings of the 2017 ACM SIGSAC Conference on Computer and Communications Security*, 2017, pp. 1175–1191.
- [27] J. H. Bell, K. A. Bonawitz, A. Gascón, T. Lepoint, and M. Raykova, "Secure single-server aggregation with (poly) logarithmic overhead," in *Proceedings of the 2020 ACM SIGSAC Conference on Computer and Communications Security*, 2020, pp. 1253–1269.
- [28] A. Cheu, A. Smith, J. Ullman, D. Zeber, and M. Zhilyaev, "Distributed differential privacy via shuffling," in *Advances in Cryptology—EUROCRYPT 2019: 38th Annual International Conference on the Theory and Applications of Cryptographic Techniques, Darmstadt, Germany, May 19–23, 2019, Proceedings, Part I 38*. Springer, 2019, pp. 375–403.
- [29] S. P. Liew, T. Takahashi, S. Takagi, F. Kato, Y. Cao, and M. Yoshikawa, "Network shuffling: Privacy amplification via random walks," in *Proceedings of the 2022 International Conference on Management*



- of Data*, ser. SIGMOD '22. New York, NY, USA: Association for Computing Machinery, 2022, p. 773–787. [Online]. Available: <https://doi.org/10.1145/3514221.3526162>
- [30] S. Takagi, F. Kato, Y. Cao, and M. Yoshikawa, “From bounded to unbounded: Privacy amplification via shuffling with dummies,” in *2023 2023 IEEE 36th Computer Security Foundations Symposium (CSF) (CSF)*. Los Alamitos, CA, USA: IEEE Computer Society, jul 2023, pp. 520–535. [Online]. Available: <https://doi.ieeecomputersociety.org/10.1109/CSF57540.2023.00034>
- [31] A. Girgis, D. Data, S. Diggavi, P. Kairouz, and A. T. Suresh, “Shuffled model of differential privacy in federated learning,” in *International Conference on Artificial Intelligence and Statistics*. PMLR, 2021, pp. 2521–2529.
- [32] J. So, R. E. Ali, B. Güler, J. Jiao, and A. S. Avestimehr, “Securing secure aggregation: Mitigating multi-round privacy leakage in federated learning,” in *Proceedings of the AAAI Conference on Artificial Intelligence*, vol. 37, no. 8, 2023, pp. 9864–9873.
- [33] D. Vatsalan, Z. Sehili, P. Christen, and E. Rahm, “Privacy-preserving record linkage for big data: Current approaches and research challenges,” *Handbook of big data technologies*, pp. 851–895, 2017.
- [34] A. Epasto, M. Mahdian, J. Mao, V. Mirrokni, and L. Ren, “Smoothly bounding user contributions in differential privacy,” *Advances in Neural Information Processing Systems*, vol. 33, pp. 13 999–14 010, 2020.
- [35] Y.-X. Wang, B. Balle, and S. P. Kasiviswanathan, “Subsampled rényi differential privacy and analytical moments accountant,” in *The 22nd International Conference on Artificial Intelligence and Statistics*. PMLR, 2019, pp. 1226–1235.
- [36] H. Yang, M. Fang, and J. Liu, “Achieving linear speedup with partial worker participation in non-iid federated learning,” *Proceedings of ICLR*, 2021.
- [37] X. Zhang, X. Chen, M. Hong, Z. S. Wu, and J. Yi, “Understanding clipping for federated learning: Convergence and client-level differential privacy,” in *International Conference on Machine Learning, ICML 2022*, 2022.
- [38] A. B. Alexandru and G. J. Pappas, “Private weighted sum aggregation,” *IEEE Transactions on Control of Network Systems*, vol. 9, no. 1, pp. 219–230, 2022.
- [39] I. Damgård, M. Geisler, and M. Krøigaard, “Efficient and secure comparison for on-line auctions,” in *Information Security and Privacy: 12th Australasian Conference, ACISP 2007, Townsville, Australia, July 2-4, 2007. Proceedings 12*. Springer, 2007, pp. 416–430.
- [40] Kaggle, “Credit card fraud detection dataset,” <https://www.kaggle.com/datasets/mlg-ulb/creditcardfraud>, 2018, accessed: 2023-08-03.
- [41] B. Balle, G. Barthe, M. Gaboardi, J. Hsu, and T. Sato, “Hypothesis testing interpretations and renyi differential privacy,” in *International Conference on Artificial Intelligence and Statistics*. PMLR, 2020, pp. 2496–2506.
- [42] F. D. McSherry, “Privacy integrated queries: an extensible platform for privacy-preserving data analysis,” in *Proceedings of the 2009 ACM SIGMOD International Conference on Management of data*, 2009, pp. 19–30.
- [43] I. Mironov, K. Talwar, and L. Zhang, “Rényi differential privacy of the sampled gaussian mechanism,” *arXiv preprint arXiv:1908.10530*, 2019.
- [44] K. Chaudhuri, J. Imola, and A. Machanavajjhala, *Capacity Bounded Differential Privacy*. Red Hook, NY, USA: Curran Associates Inc., 2019.
- [45] P. Paillier, “Public-key cryptosystems based on composite degree residuosity classes,” in *International conference on the theory and applications of cryptographic techniques*. Springer, 1999, pp. 223–238.
- [46] Z. Yang, S. Hu, and K. Chen, “Fpga-based hardware accelerator of homomorphic encryption for efficient federated learning,” *arXiv preprint arXiv:2007.10560*, 2020.
- [47] F. Mo, H. Haddadi, K. Katevas, E. Marin, D. Perino, and N. Kourtellis, “Ppfl: privacy-preserving federated learning with trusted execution environments,” in *Proceedings of the 19th annual international conference on mobile systems, applications, and services*, 2021, pp. 94–108.
- [48] F. Kato, Y. Cao, and M. Yoshikawa, “Olive: Oblivious federated learning on trusted execution environment against the risk of sparsification,” *Proc. VLDB Endow.*, vol. 16, no. 10, p. 2404–2417, aug 2023. [Online]. Available: <https://doi.org/10.14778/3603581.3603583>
- [49] S. Reddi, Z. B. Charles, M. Zaheer, Z. Garrett, K. Rush, J. Konečný, S. Kumar, and B. McMahan, Eds., *Adaptive Federated Optimization*, 2021. [Online]. Available: <https://openreview.net/forum?id=LkFG31B13U5>

## A. Omitted Statements

## 1) Definitions:

**Definition 4** (Sensitivity). *The sensitivity of a function  $f$  for any two neighboring inputs  $D, D' \in \mathcal{D}$  is:*

$$\Delta_f = \sup_{D, D' \in \mathcal{D}} \|f(D) - f(D')\|.$$

where  $\|\cdot\|$  is a norm function defined in  $f$ 's output domain.

We consider  $\ell_2$ -norm ( $\|\cdot\|_2$ ) as  $\ell_2$ -sensitivity for following analysis due to adding a Gaussian noise.

We use Rényi DP (RDP) [24] because of the tightness of the analysis of the privacy composition. The following definitions are original definitions for record-level neighboring database, but are the same for user-level neighboring database.

**Definition 5** ( $(\alpha, \rho)$ -RDP [24]). *Given a real number  $\alpha \in (1, \infty)$  and privacy parameter  $\rho \geq 0$ , a randomized mechanism  $\mathcal{M}$  satisfies  $(\alpha, \rho)$ -RDP if for any two neighboring datasets  $D, D' \in \mathcal{D}$  s.t.  $D'$  differs from  $D$  in at most one client's record set, we have that  $D_\alpha(\mathcal{M}(D) \|\mathcal{M}(D')) \leq \rho$  where  $D_\alpha(\mathcal{M}(D) \|\mathcal{M}(D'))$  is the Rényi divergence between  $\mathcal{M}(D)$  and  $\mathcal{M}(D')$  and is given by*

$$D_\alpha(\mathcal{M}(D) \|\mathcal{M}(D')) := \frac{1}{\alpha - 1} \log \mathbb{E} \left[ \left( \frac{\mathcal{M}(D)}{\mathcal{M}(D')} \right)^\alpha \right] \leq \rho,$$

where the expectation is taken over the output of  $\mathcal{M}(D)$ .

## 2) Lemmas:

**Lemma 1** (Group privacy conversion (record-level DP to GDP) [23]). *If  $f$  is  $(\epsilon, \delta)$ -DP, for any two input databases  $D, D' \in \mathcal{D}$  s.t.  $D'$  differs from  $D$  in at most  $k$  records and any subset of outputs  $Z \subseteq \mathcal{Z}$ , it holds that*

$$\Pr[f(D) \in Z] \leq \exp(k\epsilon) \Pr[f(D') \in Z] + k\epsilon^{(k-1)\epsilon} \delta.$$

It means when  $f$  is  $(\epsilon, \delta)$ -DP,  $f$  satisfies  $(k, k\epsilon, k\exp^{(k-1)\epsilon} \delta)$ -GDP.

**Lemma 2** (RDP composition [24]). *If  $\mathcal{M}_1$  satisfies  $(\alpha, \rho_1)$ -RDP and  $\mathcal{M}_2$  satisfies  $(\alpha, \rho_2)$ , then their composition  $\mathcal{M}_1 \circ \mathcal{M}_2$  satisfies  $(\alpha, \rho_1 + \rho_2)$ -RDP.*

**Lemma 3** (RDP to DP conversion [41]). *If  $\mathcal{M}$  satisfies  $(\alpha, \rho)$ -RDP, then it also satisfies  $(\rho + \log((\alpha - 1)/\alpha) - (\log \delta + \log \alpha)/(\alpha - 1), \delta)$ -DP for any  $0 < \delta < 1$ .*

**Lemma 4** (RDP Gaussian mechanism [24]). *If  $f : D \rightarrow \mathbb{R}^d$  has  $\ell_2$ -sensitivity  $\Delta_f$ , then the Gaussian mechanism  $G_f(\cdot) := f(\cdot) + \mathcal{N}(0, I\sigma^2\Delta_f^2)$  is  $(\alpha, \alpha/2\sigma^2)$ -RDP for any  $\alpha > 1$ .*

**Lemma 5** (Group-privacy of RDP (record-level DP to GDP) [24]). *If  $f : D \rightarrow \mathbb{R}^d$  is  $(\alpha, \rho)$ -RDP,  $g : D' \rightarrow D$  is  $k$ -stable and  $\alpha \geq 2^{k+1}$ , then  $f \circ g$  is  $(\alpha/2^k, 3^k \rho)$ -RDP.*

Here, group-privacy property is defined using a notion of  $k$ -stable transformation [42].  $g : D' \rightarrow D$  is  $k$ -stable if  $g(A)$  and  $g(B)$  are neighboring in  $D$  implies that there exists a

sequence of length  $c + 1$  so that  $D_0 = A, \dots, D_c = B$  and all  $(D_i, D_{i+1})$  are neighboring in  $D'$ . This privacy notion corresponds to  $(k, \cdot, \cdot)$ -GDP in Definition 2.

3) *Assumptions:* Each of these is a standard assumption in non-convex optimization. In particular, the second assumption,  $\sigma_g$ , quantifies the heterogeneity of non-i.i.d. between silos in FL and is used in many previous studies.  $\sigma_g = 0$  corresponds to the i.i.d. setting. For each  $s \in S$  and  $u \in U$ , we assume access to an unbiased stochastic gradient  $g_{t,q}^{s,u}$  of the true local gradient  $\nabla f_{s,u}(x)$  for  $s$  and  $u$ .

**Assumption 1** (Lipschitz Gradient). *The function  $f_{s,u}$  is  $L$ -smooth for all silo  $s \in S$  and user  $u \in U$ , i.e.,  $\|\nabla f_{s,u}(x) - \nabla f_{s,u}(y)\| \leq L\|x - y\|$ , for all  $x, y \in \mathbb{R}^d$ .*

**Assumption 2** (Bounded Local and Global Variance). *The function  $f_{s,u}$  is  $\sigma_l$ -locally-bounded, i.e., the variance of each local gradient estimator is bounded as  $\mathbb{E}[\|g_{t,q}^{s,u} - \nabla f_{s,u}(x_{t,q}^{s,u})\|^2] \leq \sigma_l^2$  for all  $s, u$  and  $t, q$ . And the functions are  $\sigma_g$ -globally-bounded, i.e., the global gradient variance is bounded as  $\|\nabla f_{s,u}(x_t) - \nabla f_{s,u}(x_t)\|^2 \leq \sigma_g^2$  for all  $s, u, t$ .*

**Assumption 3** (Globally Bounded Gradients). *For all  $s, u, t, q$ , gradient is  $G$ -bounded, i.e.,  $\|g_{t,q}^{s,u}\| \leq G$ .*

4) *Algorithms:* Algorithm 3 provides a detailed description of ULDP-NAIVE, Algorithm 4 shows ULDP-SGD. The details of the algorithm of ULDP-AVG with user-level subsampling is shown in Algorithm 5. The difference from ULDP-AVG highlights in red letters. Algorithm 6 shows ENCODE and DECODE that are used in the private weighting protocol described in Protocol B. These are used for conversions from floating-point values to fixed-point values to be handled on a finite field, and vice versa.

## 5) Proofs:

**Proof of Theorem 1**

*Proof.* At the round  $t$ , due to the clipping operation (Line 14 in Algorithm 3), for each  $s \in S$  any user's contribution to  $\Delta_t^s$  (Line 6) is limited to at most  $C$  (regardless of the number of user records). And since a single user may exist in any silo, he/she contributes at most  $|S|C$  to  $\sum_{s \in S} \Delta_t^s$ , which means user-level sensitivity is  $|S|C$ . Therefore, when the each silo adds the Gaussian noise with variance  $\sigma^2 C^2 |S|$ ,  $\sum_{s \in S} \Delta_t^s$  includes the Gaussian noise with variance  $\sigma^2 C^2 |S|^2$ . Then, by Lemma 4, it satisfies  $(\alpha, \frac{\alpha}{2\sigma^2})$ -RDP for  $\alpha > 1$ . And after  $T$  rounds, it satisfies  $(\alpha, \frac{T\alpha}{2\sigma^2})$ -RDP by Lemma 2. Finally, by Lemma 3, we get the final result.  $\square$

**Proof of Theorem 2**

*Proof.* In each silo  $s \in S$ , by DP-SGD with  $Q$  epochs and  $T$  rounds, we have record-level  $(\alpha, \rho_s = \rho(\sigma, \gamma, QT))$ -RDP. The actual value of  $\rho_s$  is calculated numerically as described in [43]. RDP is known to satisfy parallel composition [44]. That is, for disjoint database  $D_1$  and  $D_2$ , their combined release  $(\mathcal{M}_1(D_1), \mathcal{M}_2(D_2))$  such that  $\mathcal{M}_1$  with  $(\alpha, \rho_1)$ -RDP and  $\mathcal{M}_2$  with  $(\alpha, \rho_2)$ -RDP satisfies  $(\alpha, \max\{\rho_1, \rho_2\})$ -RDP. For any silo  $s \in S$ , input database  $D_s$  is disjoint with

---

**Algorithm 3** ULDP-NAIVE

---

**Input:**  $S$ : silo set (silo  $s \in S$ ),  $\eta_l$ : local learning rate,  $\eta_g$ : global learning rate,  $\sigma$ : noise parameter,  $C$ : clipping bound,  $T$ : total round,  $Q$ : #local epochs

```
1: procedure SERVER
2:   Initialize model  $x_0$ 
3:   for each round  $t = 0, 1, \dots, T - 1$  do
4:     for each silo  $s \in S$  do
5:        $\Delta_t^s \leftarrow \text{CLIENT}(x_t, C, \sigma, \eta_l)$ 
6:        $x_{t+1} \leftarrow x_t + \eta_g \frac{1}{|S|} \sum_{s \in S} \Delta_t^s$ 
7:   procedure CLIENT( $x_t, C, \sigma, \eta_l$ )
8:      $x_s \leftarrow x_t$ 
9:     for epoch  $q = 0, 1, \dots, Q - 1$  do
10:      Compute stochastic gradients  $g_{t,q}^{(s)}$ 
11:       $\triangleright \mathbb{E}[g_{t,q}^{(s)}] = \nabla f_s(x_s)$ 
12:       $x_s \leftarrow x_s - \eta_l g_{t,q}^{(s)}$ 
13:       $\tilde{\Delta}_t \leftarrow x_t - x_s$ 
14:       $\tilde{\Delta}_t \leftarrow \tilde{\Delta}_t \cdot \min\left(1, \frac{C}{\|\tilde{\Delta}_t\|_2}\right)$   $\triangleright$  clipping with  $C$ 
15:       $\Delta_t' \leftarrow \tilde{\Delta}_t + \mathcal{N}(0, I\sigma^2 C^2 |S|)$ 
16:      return  $\Delta_t'$ 
```

---

---

**Algorithm 4** ULDP-SGD

---

**Input:**  $U$ : user set (user  $u \in U$ ),  $S$ : silo set (silo  $s \in S$ ),  $\eta_g$ : global learning rate,  $\sigma$ : noise parameter,  $C$ : clipping bound,  $T$ : total round,  $\mathbf{W} = (\mathbf{w}_1, \dots, \mathbf{w}_{|S|})$ : matrix with weight for user  $u$  and silo  $s$ , and  $\forall u \in U, w_{s,u} \in \mathbf{w}_s$  and  $\sum_{s \in S} w_s^{(u)} = 1$

```
1: procedure SERVER
2:   Initialize model  $x_0$ 
3:   for each round  $t = 0, 1, \dots, T - 1$  do
4:     for each silo  $s \in S$  do
5:        $g_t^s \leftarrow \text{CLIENT}(x_t, \mathbf{w}_s, C, \sigma)$ 
6:        $x_{t+1} \leftarrow x_t - \eta_g \frac{1}{|U||S|} \sum_{s \in S} g_t^s$ 
7:   procedure CLIENT( $x_t, \mathbf{w}_s, C, \sigma$ )
8:     for user  $u \in U$  do  $\triangleright$  per-user training
9:       Compute stochastic gradients  $g_t^{s,u}$ 
10:       $\triangleright \mathbb{E}[g_t^{s,u}] = \nabla f_{s,u}(x_s)$ 
11:       $\tilde{g}_t^{s,u} \leftarrow w_{s,u} \cdot g_t^{s,u} \cdot \min\left(1, \frac{C}{\|g_t^{s,u}\|_2}\right)$ 
12:       $\tilde{g}_t^s \leftarrow \sum_{u \in U} \tilde{g}_t^{s,u} + \mathcal{N}(0, I\sigma^2 C^2 / |S|)$ 
13:      return  $\tilde{g}_t^s$ 
```

---

others. Therefore, after  $T$  rounds, the trained model satisfies  $(\alpha, \rho = \max_{s \in S} \rho_s)$ -RDP for across silo entire database  $D = D_1 \oplus \dots \oplus D_{|S|}$ . Then, by Lemma 5 and Lemma 3, for any integer  $k$  to the power of 2 and any  $\alpha \geq 2^{k+1}$ , it also satisfies  $(k, 3^k \rho + \log((\frac{\alpha}{2^k} - 1)/\frac{\alpha}{2^k}) - (\log \delta + \log \frac{\alpha}{2^k})/(\frac{\alpha}{2^k} - 1), \delta)$ -GDP. Finally, by filtering with  $\mathbf{B}$ , we guarantee that any user has at most  $k$  records in  $D$ . Finally, we get the final result by Proposition 1. (Another method to compute  $\epsilon$  is to use Lemma 1 instead of Lemma 5.)  $\square$

---

**Algorithm 5** ULDP-AVG with user-level sub-sampling

---

**Input:**  $U$ : user set (user  $u \in U$ ),  $S$ : silo set (silo  $s \in S$ ),  $\eta_l$ : local learning rate,  $\eta_g$ : global learning rate,  $\sigma$ : noise parameter,  $C$ : clipping bound,  $T$ : total round,  $Q$ : #local epochs,  $\mathbf{W} = (\mathbf{w}_1, \dots, \mathbf{w}_{|S|})$ : matrix with weight for user  $u$  and silo  $s$ , and  $\forall u \in U, w_{s,u} \in \mathbf{w}_s$  and  $\sum_{s \in S} w_{s,u} = 1$ ,  $q$ : user-level sub-sampling probability

```
1: procedure SERVER
2:   Initialize model  $x_0$ 
3:   for each round  $t = 0, 1, \dots, T - 1$  do
4:      $U_t \leftarrow \text{Poisson sampling from } U \text{ with probability } q$ 
5:     for each silo  $u \in U_t$  do
6:       for each silo  $s \in S$  do
7:          $w_{s,u} \leftarrow 0$ 
8:       for each silo  $s \in S$  do
9:          $\Delta_t^s \leftarrow \text{CLIENT}(x_t, \mathbf{w}_s, C, \sigma, \eta_l)$ 
10:       $x_{t+1} \leftarrow x_t + \eta_g \frac{1}{|U||S|} \sum_{s \in S} \Delta_t^s$ 
11:   procedure CLIENT( $x_t, \mathbf{w}_s, C, \sigma, \eta_l$ )
12:     for user  $u \in U$  do  $\triangleright$  per-user training
13:        $x_t^{s,u} \leftarrow x_t$ 
14:       for epoch  $q = 0, 1, \dots, Q - 1$  do
15:         Compute stochastic gradients  $g_{t,q}^{s,u}$ 
16:          $\triangleright \mathbb{E}[g_{t,q}^{s,u}] = \nabla f_{s,u}(x_t^{s,u})$ 
17:          $x_t^{s,u} \leftarrow x_t^{s,u} - \eta_l g_{t,q}^{s,u}$ 
18:          $\Delta_t^{s,u} \leftarrow x_t^{s,u} - x_t$ 
19:          $\tilde{\Delta}_t^{s,u} \leftarrow w_{s,u} \cdot \Delta_t^{s,u} \cdot \min\left(1, \frac{C}{\|\Delta_t^{s,u}\|_2}\right)$   $\triangleright$  per-user weighted clipping
20:          $\tilde{\Delta}_t^s \leftarrow \sum_{u \in U} \tilde{\Delta}_t^{s,u} + \mathcal{N}(0, I\sigma^2 C^2 / |S|)$ 
21:         return  $\tilde{\Delta}_t^s$ 
```

---

**Proof of Theorem 3**

*Proof.* For any round  $t$ , due to the clipping operation (Line 15), for each  $s \in S$  any user's contribution to  $\Delta_t^s$  (Line 6) is limited to at most  $w_{s,u}C$  (regardless of the number of user records). Therefore, for  $\sum_{s \in S} \Delta_t^s$  (Line 6), any user's contribution is at most  $\sum_{s \in S} w_{s,u}C = C$  since  $\sum_{s \in S} w_{s,u} = 1$ . That means the user-level sensitivity is just  $C$ . And since the each silo adds the Gaussian noise with variance  $\sigma^2 C^2 / |S|$ ,  $\sum_{s \in S} \Delta_t^s$  includes Gaussian noise with variance  $\sigma^2 C^2$ . Then, by Lemma 4, it satisfies  $(\alpha, \frac{\alpha}{2\sigma^2})$ -RDP for  $\alpha > 1$  in a user-level manner. And after  $T$  rounds, it satisfies  $(\alpha, \frac{T\alpha}{2\sigma^2})$ -RDP by Lemma 2. Finally, by Lemma 3, we get the result.  $\square$

**B. Details of private weighting protocol**

The details of the private weighting protocol are explained in Protocol 1. Our protocol consists of a setup phase, which is executed only once during the entire training process, and a weighting phase, which is executed in each round of training. In the setup phase, as depicted in (a-c) of Protocol 1, the server generates a keypair for Paillier encryption, while the silos establish shared random seeds through a Diffie-Hellman

---

**Protocol 1** Private Weighting Protocol

*Inputs:* Silo  $s \in S$  that holds an dataset with  $n_{s,u}$  records for each user  $u \in U$ .  $\mathcal{A}$  is central aggregation server.  $N_{\max}$  is upper bound on the number of records per user, e.g., 2000.  $P$  is precision parameter, e.g.,  $10^{-10}$ .  $\lambda$  is security parameter, e.g., 3072-bit security.

**1) Setup.**

- a)  $\mathcal{A}$  generates Paillier keypairs  $(PK, SK)$  with the given security parameter  $\lambda$  and sends the public key  $PK$  to all silos. All  $s$  generate DH keypairs  $(pk_s, sk_s)$  with the same parameter  $\lambda$  and transmit their respective public key  $pk_s$  to  $\mathcal{A}$ . Both  $\mathcal{A}$  and all silos compute  $C_{\text{LCM}}$  which is the least common multiple of all integers up to  $N_{\max}$ . The modulus  $n$  included in  $PK$  is used for finite field  $\mathbb{F}_n$  by  $\mathcal{A}$  and all silos.
- b) After receiving all  $pk_s$ ,  $\mathcal{A}$  broadcasts all DH public keys  $pk_s$  to all  $s$ . All  $s$  compute shared keys  $sk_{s,s'}$  from  $sk_s$  and received public keys  $pk_{s'}$  for all  $s' \in S$ .
- c) Silo 0 ( $\in S$ ) generates a random seed  $R$  and encrypts  $R$  using  $sk_{0,s'}$  to obtain  $Enc(R)$  and sends  $Enc(R)$  to  $s'$  via  $\mathcal{A}$  for all  $s'$ . All  $s \in S \setminus 0$  receive and decrypt  $Enc(R)$  with  $sk_{s,0}$  and get  $R$  as a shared random seed.
- d) All  $s$  generate multiplicative blind masks  $r_u \in \mathbb{F}_n$  with the same  $R$  and compute blinded histogram as  $B(n_{s,u}) \equiv r_u n_{s,u} \pmod{n}$  for all  $u \in U$ .
- e) All  $s$  generate pair-wise additive masks  $r_{s,s'}^u \in \mathbb{F}_n$  employing  $sk_{s,s'}$  for all  $s'$  and  $u$ , with  $r_{s,s'}^u = r_{s',s}^u$ . Subsequently, they calculate the doubly blinded histogram as  $B'(n_{s,u}) \equiv B(n_{s,u}) + \sum_{s < s'} r_{s,s'}^u - \sum_{s > s'} r_{s,s'}^u \pmod{n}$ . All  $s$  send  $B'(n_{s,u})$  to  $\mathcal{A}$ .  $\mathcal{A}$  aggregates these contributions to compute  $B(N_u) \equiv \sum_{s \in S} B'(n_{s,u}) \pmod{n}$  for each  $u$ , denoting  $N_u = \sum_{s \in S} n_{s,u}$ .
- f)  $\mathcal{A}$  computes the inverse of  $B(N_u)$  as  $B_{\text{inv}}(N_u) = B(N_u)^{-1}$  for each  $u$ . This is the multiplicative inverse on  $\mathbb{F}_n$ , which is efficiently computed by the Extended Euclidean algorithm.

**2) Weighting for each training round  $t$ .**

- a)  $\mathcal{A}$  encrypts  $B_{\text{inv}}(N_u)$  using Paillier's public key  $PK$ , resulting in  $Enc_p(B_{\text{inv}}(N_u))$  for all  $u$ . If user-level sub-sampling is required, the server performs Poisson sampling with a given probability  $q$  for each user before the encryption. For non-selected users,  $B_{\text{inv}}(N_u)$  is set to 0. If we require user-level sub-sampling, we perform Poisson sampling with given probability  $q$  on the server for each user before the Paillier's encryption and set  $B_{\text{inv}}(N_u) = 0$  for all users not selected. Subsequently,  $\mathcal{A}$  broadcasts all  $Enc_p(B_{\text{inv}}(N_u))$  to all silos.
- b) In each  $s$ , following the approach of ULDP-AVG, the clipped model delta  $\tilde{\Delta}_t^{s,u}$  is computed for each user  $u$ . The weighted clipped model delta is then calculated as

$$Enc_p(\tilde{\Delta}_t^{s,u}) = \text{ENCODE}(\tilde{\Delta}_t^{s,u}, P, n) n_{s,u} r_u C_{\text{LCM}} Enc_p(B_{\text{inv}}(N_u)).$$

Let the Gaussian noise be  $z_t^s$ , we then compute  $z'_s = \text{ENCODE}(z_t^s, P, n) C_{\text{LCM}}$ . Note that we need to approximate real number  $\tilde{\Delta}_t^{s,u}$  and  $z_t^s$  on a finite field using ENCODE (described in Algorithm 6). Lastly, we compute the summation  $Enc_p(\Delta_t^s) = \sum_{u \in U} Enc_p(\tilde{\Delta}_t^{s,u}) + z'_s$ .

- c) In each  $s$ , random pair-wise additive masks are generated, and secure aggregation is performed on  $Enc_p(\Delta_t^s)$  mirroring the steps in 1.(f). Then,  $\mathcal{A}$  gets  $\sum_{s \in S} Enc_p(\Delta_t^s)$ .  $\mathcal{A}$  decrypts it with Paillier's secret key  $SK$  and decodes it by  $\text{DECODE}(\sum_{s \in S} \Delta_t^s, P, C_{\text{LCM}}, n)$  and recovers the aggregated value.
- d) Steps 2.(a) through 2.(c) are repeated for each training round.

---

**Algorithm 6** ENCODE and DECODE functions in the private weighting protocol

---

```

1: procedure ENCODE( $x, P, n$ )           ▷ e.g.,  $P = 10^{-10}$ 
2:   /* to turn floating point into fixed point */
3:    $x \leftarrow x/P$                    ▷ compute as floating point
4:    $x \leftarrow x$  as integer
5:   /* to map integer  $\mathbb{Z}$  into finite field  $\mathbb{F}_n$  */
6:    $x \leftarrow x \pmod{n}$ 
7:   return  $x$ 

8: procedure DECODE( $x, P, C_{\text{LCM}}, n$ )
9:   /* to map finite field  $\mathbb{F}_n$  number into integer  $\mathbb{Z}$  */
10:  if  $x > n//2$  then                 ▷ // means integer division
11:     $x \leftarrow x - n$ 
12:  else
13:     $x \leftarrow x$ 
14:  /* to remove  $C_{\text{LCM}}$  factor */
15:   $x \leftarrow x/C_{\text{LCM}}$              ▷ compute as floating point
16:  /* to recover original magnitude */
17:   $x \leftarrow xP$ 
18:  return  $x$ 

```

---

(DH) key exchange via the server. Subsequently, (d-f) the blinded inverses of the user histogram are computed. In the weighting phase, (a) the server prepares the encrypted weights, (b) the silos compute user-level weighted model deltas in the encrypted world, and (c) the server recovers the aggregated value. It's important to note that in the Paillier cryptosystem, the plaintext data  $x$  exists within the additive group modulo  $n$ , while encrypted data (denoted as  $Enc_p(x)$ ) belongs to the multiplicative group modulo  $n^2$  with an order of  $n$ . The system allows for operations such as addition of ciphertexts and scalar multiplication and addition of ciphertexts.

We provide a theoretical analysis of this private weighting protocol in terms of correctness and privacy as outlined below.

1) *Correctness:* The protocol must compute the correct result as the same result as non-secure method. To this end, we consider the correctness of the aggregated data obtained in each round. Let  $\sum_{s \in S} \Delta_t^s$  with non-secure method be  $\Delta$  and the one with the Protocol 1 be  $\Delta_{\text{sec}}$ , our goal is formally stated as  $\Pr[|\Delta - \Delta_{\text{sec}}|_{\infty} > P] < \text{negl}$ , where  $P$  is a precision parameter and *negl* signifies a negligible value.

Initially, with regards to secure aggregation, the additive pair-wise masks cancel out as shown in [26]. For the difference, silo must participate in any rounds in our cross-silo FL. When collecting the histogram, additive masks are canceled out as follows:

$$B(N_u) = \sum_{s \in S} B(n_{s,u}) + \sum_{s < s'} \underbrace{(r_{s,s'}^u - r_{s',s}^u)}_{\text{canceled out}} - \sum_{s > s'} \underbrace{(r_{s,s'}^u - r_{s',s}^u)}_{\text{canceled out}}$$

The same applies to secure aggregation for model delta. Note that the mask is not directly added to the ciphertext (within

the multiplication group of  $n^2$ ); instead scalar addition within  $\mathbb{F}_n$  that takes advantage of homomorphic property of Paillier cryptosystem is utilized. As secure aggregation doesn't result in any degradation of the aggregation outcome when all terms are within  $\mathbb{F}_n$ , our focus shifts to other components. Note that there are errors due to the handling of fixed-point numbers on a finite field.

From the protocol description,  $Enc_p(\Delta_{\text{sec}})$  is analyzed as follows:

$$\begin{aligned}
Enc_p(\Delta_{\text{sec}}) &= \sum_{s \in S} Enc_p(\Delta_t^s) = \sum_{s \in S} \sum_{u \in U} Enc_p(\tilde{\Delta}_t^{s,u}) + z'_s \\
&= \sum_{s \in S} \sum_{u \in U} E_t^{s,u} n_{s,u} r_u C_{\text{LCM}} Enc_p(B_{\text{inv}}(N_u)) + Z_t^s C_{\text{LCM}} \\
&\stackrel{(1)}{=} Enc_p\left(\sum_{s \in S} \left(\sum_{u \in U} (E_t^{s,u} n_{s,u} r_u C_{\text{LCM}} B_{\text{inv}}(N_u))\right) + Z_t^s C_{\text{LCM}}\right) \\
&= Enc_p\left(\sum_{s \in S} \left(\sum_{u \in U} (E_t^{s,u} n_{s,u} r_u C_{\text{LCM}} (r_u N_u)^{-1}) + Z_t^s C_{\text{LCM}}\right)\right) \\
&\stackrel{(2)}{=} Enc_p\left(\sum_{s \in S} \left(\sum_{u \in U} (E_t^{s,u} n_{s,u} C_{-N_u}) + Z_t^s C_{\text{LCM}}\right)\right)
\end{aligned}$$

where  $C_{-N_u}$  is the result of modular multiplication between  $C_{\text{LCM}}$  and the modular multiplicative inverse of  $N_u$ ,  $E_t^{s,u} = \text{ENCODE}(\tilde{\Delta}_t^{s,u}, P, n)$  and  $Z_t^s = \text{ENCODE}(z_t^s, P, n)$ . Equation (1) is because all of  $B_{\text{inv}}$ ,  $E_t^{s,u}$ ,  $n_{s,u}$ ,  $r_u$  and  $C_{\text{LCM}} \in \mathbb{F}_n$ . At (2), the modulo inverse of  $r_u$  is canceled out because  $r_u \in \mathbb{F}_n$  and  $r_u$  almost always has modulo inverse. However, this does not hold when  $r_u$  and  $n$  are not coprime. Let  $p$  and  $q$  be two large primes used in the Paillier cryptosystem, such that  $n = pq$ , then the probability of a random  $r_u \in \mathbb{F}_n$  and  $n$  are not coprime is

$$\frac{n-1-\phi(n)}{n-1} = \frac{n-1-(p-1)(q-1)}{n-1}, \quad (5)$$

where  $\phi$  is Euler's totient function. This probability is negligibly small when  $n$  is sufficiently large. In the case of user-level sub-sampling,  $B_{\text{inv}}(N_u)$  is set 0 and we see that only the model delta for user  $u$  is all zeros, which produces exactly the same result as if the unselected users did not participate in the training round. The important condition is that if  $N_u \leq N_{\text{max}}$  and  $N_u$  is a factor of  $C_{\text{LCM}}$ ,  $C_{\text{LCM}}/N_u$  is always divisible on  $\mathbb{Z}$  and the result is the same as on  $\mathbb{F}_n$ . Also if  $\sum_{s \in S} (\sum_{u \in U} (E_t^{s,u} n_{s,u} C_{-N_u}) + Z_t^s C_{\text{LCM}}) \in \mathbb{Z}$  is smaller than  $n$ , it yields the same results on  $\mathbb{Z}$  and  $\mathbb{F}_n$ . Hence, when these conditions are satisfied, decrypted value  $\Delta_{\text{sec}} \in \mathbb{F}_n$  obtains the same result on  $\Delta_{\text{sec}} \in \mathbb{Z}$ . After decryption, we consider  $\Delta_{\text{sec}} \in \mathbb{R}$ . The final result is decoded by  $\text{DECODE}(\Delta_{\text{sec}}, P, C_{\text{LCM}}, n) \in \mathbb{R}$  as follows:

$$\text{DECODE}(\Delta_{\text{sec}}, P, C_{\text{LCM}}, n) = \sum_{s \in S} \left(\sum_{u \in U} \left(\frac{n_{s,u}}{N_u} \tilde{\Delta}'_{s,u,t}\right) + Z'_{s,t}\right)$$

where, from Algorithm 6,  $\tilde{\Delta}'_{s,u,t}$  is the same as the result of computing  $\tilde{\Delta}_t^{s,u}$  in fixed-point with precision  $P$ , and  $Z'_{s,t}$  is the same as  $z_t^s$ .

Therefore, the correctness of these calculations is satisfied when two conditions (1)  $N_u \leq N_{\text{max}}$  and (2)

$\sum_{s \in S} (\sum_{u \in U} (E_t^{s,u} n_{s,u} C_{-N_u}) + Z_t^s C_{\text{LCM}}) < n$ , are satisfied. To satisfy (1),  $N_{\text{max}}$  must be sufficiently large, and a larger  $N_{\text{max}}$  leads to a larger  $C_{\text{LCM}}$ . Hence, when we take  $n$  is large, these conditions can be satisfied unless the parameters or noise take on unrealistic values.

For example, suppose the range of the noise and aggregated model parameters is  $[-10^{10}, 10^{10}]$ ,  $P = 10^{-10}$ ,  $N_{\text{max}} = 2000$  and  $\lambda$  is 3072-bit security, we have  $n > 10^{924}$  by Paillier cryptosystem,  $E_t^{s,u} < 10^{20}$ ,  $Z_t^s < 10^{20}$  and  $C_{\text{LCM}} < 10^{867}$ . Then,  $\sum_{s \in S} (\sum_{u \in U} (E_t^{s,u} n_{s,u} C_{-N_u}) + Z_t^s C_{\text{LCM}}) < 10^{888} < n$  and we satisfy the condition (2).  $C_{\text{LCM}}$  grows exponentially with respect to  $N_{\text{max}}$ . One possible solution for this is that we can make it very small by limiting the number of records per user to several values. For example,  $\{10^1, 10^2, 10^3, 10^4\}$  then  $C_{\text{LCM}} = 10^4$ .

2) *Privacy*: Privacy in this protocol means that both the central server and the silos do not get more information than is available in the original ULDP-AVG while we perform the better weighting strategy. Our approach relies on a private weighted sum aggregation technique employing the Paillier cryptosystem [19], [45] and secure aggregation [26]. Formal security arguments for these methodologies are available in their respective sources. Our protocol is fully compatible with these works because all data exchanged is handled on  $\mathbb{F}_n$  including random masks for secure aggregation.

A different view of the server from these basic methods is  $B(N_u)$  for all  $u$  which is multiplicatively blinded aggregated histogram. Since  $B(n_{s,u})$  for  $s$  and  $u$  is securely hidden by secure aggregation, only  $B(N_u)$  is the meaningful server view.  $B(N_u)$  is  $r_u N_u \pmod{n}$  and this is randomly distributed on  $\mathbb{F}_n$  if  $r_u$  is uniformly distributed on  $\mathbb{F}_n$ . Also, the inverse of  $B_{\text{inv}}(N_u)$  is uniformly distributed as well. This is because the multiplication operation in a finite field is closed and bijective. Therefore, it is information-theoretically indistinguishable and private. Such multiplicative blinding has been also used in [39]. The view of the silos is the same as that of [19] even though the contents of the weights are sensitive, and privacy is protected by Paillier encryption. Note that the security of the initial DH key exchange and the security of the Paillier cryptosystem follows the security parameter  $\lambda$ , which is the protocol input.

### C. Omitted Figures

We illustrate an intuitive difference between ULDP-NAIVE and ULDP-AVG in Figure 6. In ULDP-NAIVE, every single user can contribute to all model deltas. On the other hand, in ULDP-AVG, one user's contribution is limited to a small portion, i.e.,  $1/|U|$  of the whole model delta. This reduces sensitivity. When  $|U|$  is large, which often happens in cross-silo FL, it can be a particular advantage.

### D. Omitted Experiments and details

For ease of access, all of our experimental code and datasets are available at the open repository: <https://github.com/FumiyukiKato/uldp-fl>.

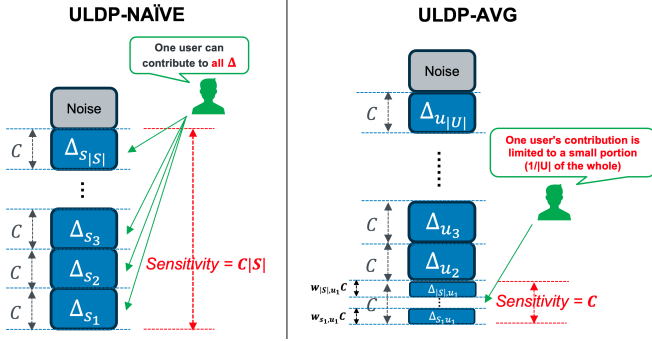


Fig. 6: An intuitive illustration of the difference between ULDP-NAIVE and ULDP-AVG. In ULDP-NAIVE, every single user can contribute to all model deltas. On the other hand, in ULDP-AVG, one user’s contribution is limited to a small portion, i.e.,  $1/|U|$  of the whole model delta. This reduces sensitivity. When  $|U|$  is large, which often happens in cross-silo FL, it can be a particular advantage.

1) *GDP comparison: RDP vs Normal DP*: For the experiment in Figure 2, we ran the Gaussian mechanism with  $\sigma = 5.0$  and sampling rate = 0.01 for  $10^5$  iterations, which emulates a typical DP-SGD execution setup. We use fixed  $\delta = 10^{-5}$  and varies group size  $k = 1, 2, 4, 8, 16, 32, 64$ .

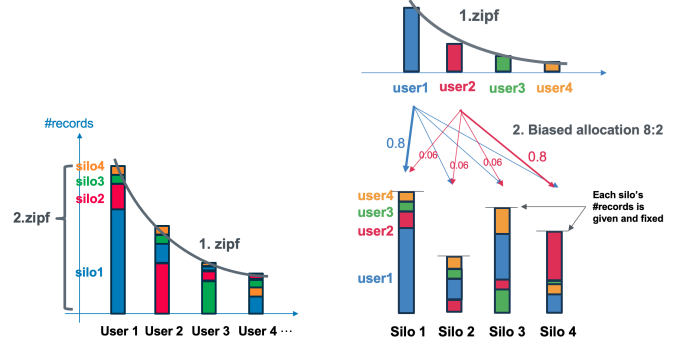
To compute GDP, RDP for sub-sampled Gaussian mechanism was calculated according to [35]. Then, for group-privacy of RDP, we compute GDP by Lemma 5.

For normal DP, the computed RDP is converted to normal DP by Lemma 3, and then converted to GDP by Lemma 1. When converting to normal DP to GDP, computing final  $\epsilon$  at fixed  $\delta$  is not easy. In Lemma 3, output  $\epsilon$  (denoting  $\epsilon_3$ ) depends on input  $\delta$  (denoting  $\delta_3$ ), and the final  $\delta$  (denoting  $\delta_1$ ) output by Lemma 1 depends on the  $\epsilon_3$  and  $\delta_3$ . Therefore, we repeatedly select  $\delta_3$  in a binary search manner, and compute  $\epsilon_3$  and  $\delta_3$ , and finally report the  $\epsilon$  when difference of  $\delta_3$  and  $\delta = 10^{-5}$  are sufficiently small (accuracy by  $10^{-8}$ ) as the  $\epsilon$  of GDP. The implementation is a function `get_normal_group_privacy_spent()` in [https://github.com/FumiyukiKato/uldp-fl/blob/main/src/noise\\_utils.py](https://github.com/FumiyukiKato/uldp-fl/blob/main/src/noise_utils.py).

Note that there is no guarantee that this method will achieve optimal  $\epsilon$  with given  $\delta$  but find reasonable  $\epsilon$ .

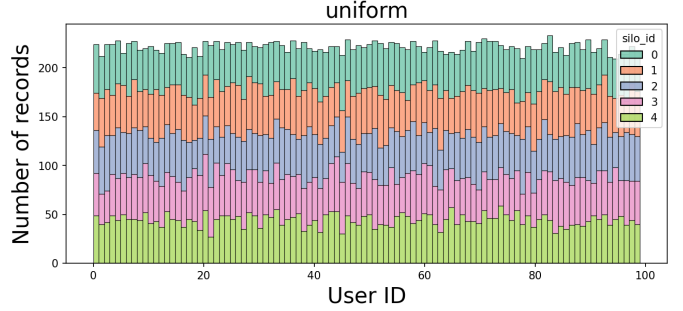
2) *Record allocation: MNIST and Creditcard*. We designed two different record distribution patterns, *uniform* and *zipf*, to model how user records are scattered across silos in the MNIST and Creditcard datasets. Both distributions take the number of users  $|U|$  and the number of silos  $|S|$ . It associates each record with a user and a silo.

(1) In uniform, every record is assigned to a user with equal probability, and likewise, each record is assigned to a silo with equal probability. (2) *zipf* combines two types of Zipf distributions as shown in Figure 7a. First, the distribution of the number of records per user follows a Zipf distribution. Then, for each user, the numbers of records are assigned to different silos based on another Zipf distribution. Each of

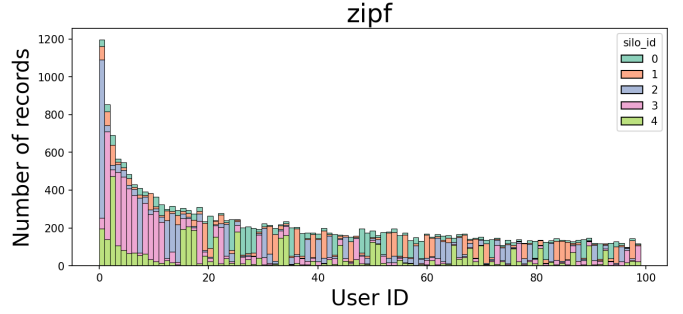


(a) MNIST and Creditcard. (b) HeartDisease and TcgaBrca.

Fig. 7: Record distribution across users and silos.



(a) uniform.



(b) zipf.

Fig. 8: Example of record allocation on Creditcard.

the two Zipf distributions takes a parameter  $\alpha$  that determines the concentration of the numbers. In our experiments, we used  $\alpha = 0.5$  for the first distribution and  $\alpha = 2.0$  for the second distribution. This choice is rooted in the observation that the concentration of user records is not as high as the concentration in the silos selected by each user.

For Creditcard and MNIST, the number of silos  $|S|$  is fixed at 5. We used 100, 1000 for Creditcard as  $|U|$  and 100, 10000 for MNIST. For MNIST, we can require each user to have only 2 labels at most in the non-i.i.d. setting. For example, when  $|U| = 100$  and  $|S| = 5$ , the record distribution of Creditcard dataset is shown in Figure 8. The number of records is plotted for each user and color-coded for each silo.

**HeartDisease and TcgaBrca**. For the HeartDisease and TcgaBrca datasets, we adopted the same two distributions

*uniform* and *zipf* as above-mentioned ones. In, the benchmark datasets HeartDisease and TcgaBrca, all records are already allocated to silos and the number of records of each silo is fixed. Therefore, the design of the user-record allocation is slightly different.

(1) In *uniform*, all records belong to one of the users with equal probability without allocation to silos. (2) In *zipf*, as shown in Figure 7b, the number of records for a user is first generated according to a Zipf distribution, and 80% of the records are assigned to one silo, and the rest to the other silos with equal probability. The priority of the silo is chosen randomly for each user.  $\alpha = 0.5$  was used for the parameter of the Zipf. In TcgaBrca, Cox-Loss is used for loss function [18], which needs more than two records for calculating valid loss and we set more than two records for each silo and user for per-user clipping of ULDP-AVG.

3) *Hyperparameters*: All scripts used in the experiments, including hyperparameters, can be accessed here: [https://github.com/FumiyukiKato/uldp-fl/blob/main/exp/script/privacy\\_utility.sh](https://github.com/FumiyukiKato/uldp-fl/blob/main/exp/script/privacy_utility.sh).

4) *Additional experiments*: We provide additional experimental results to support the claims made in the paper. In addition to the three dataset mentioned in the paper, we evaluate our method on a well-known image dataset MNIST. For MNIST, we use a CNN model about 20K parameters, 60K training data and 10K evaluation data, and assigned silos and users to all of the training data. The default setting of all of the following experiments is the same as specified in the paper.

**Privacy-utility trade-offs under ULDP.** Figure 9, 10 and 11 shows a privacy-utility trade-offs on HeartDisease, TcgaBrca and MNIST, respectively. All experiments used a fixed noise parameter (noise multiplier)  $\sigma = 5.0$  and  $\delta = 10^{-5}$ , utility metrics (Accuracy for HeartDisease and MNIST, C-index for TcgaBrca) are plotted in left side and accumulated privacy consumption  $\epsilon$  for ULDP are plotted in right side. For clarity, the test loss is shown on the left hand side on MNIST. The average number of records per user (denoting as  $n$ ) in entire silos and the distribution (uniform/zipf) changes for each figure.

In all datasets, consistently, ULDP-AVG is competitive in terms of utility, ULDP-AVG-w shows much faster convergence, and ULDP-SGD shows slower convergence. ULDP-NAIVE achieves low privacy bound; however, its utility is much lower than other methods. The group-privacy methods such as ULDP-GROUP- $k$  show reasonably high utility especially in settings where  $n$  is small. This is because the records to be removed due to the number of records per user being over group size  $k$  is small. However, the ULDP privacy bound ULDP-GROUP- $k$  achieves ends up being very large. Note that the privacy bounds for ULDP-GROUP- $k$  are derived from the local DP-SGD and depend on not only the group size  $k$  but also the size of the local training dataset. The exceptions are cases where the local data set size is large and the number of records per user is very small as Figures 11d, 11e and 11f. In these case, ULDP-GROUP-2 achieves a reasonably small privacy bound. In other words, if the number of user records is

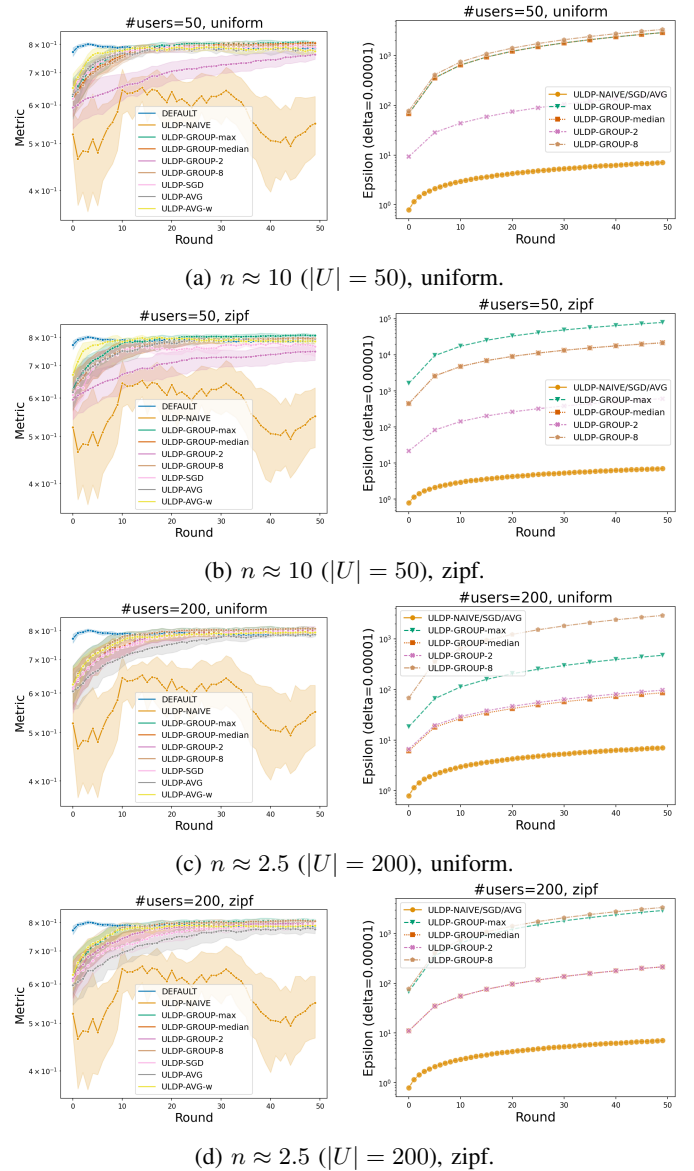


Fig. 9: Privacy-utility trade-offs on HeartDisease dataset. Test Accuracy (Left), Privacy (Right).

fixed at one or two in the scenario, and the number of training records is large (it is advantageous for ULDP-GROUP because the record-level sub-sampling rate in DP-SGD becomes small), it could be better to use ULDP-GROUP.

The results for the MNIST, non-i.i.d and  $|U| = 100$  case highlight a weak point of ULDP-AVG. Note that non-i.i.d here is at user-level and DEFAULT and ULDP-GROUP are less affected by non-i.i.d because they do train per silo rather than per user. As Figure 11c shows, the convergence of ULDP-AVG is worse compared to other results. It suggests that ULDP-AVG may emphasize the bad effects of user-level non-i.i.d. distribution that were not an issue with normal cross-silo FL because the gradient is not computed at the user level as in ULDP-AVG. On the other hand, this is less problematic when

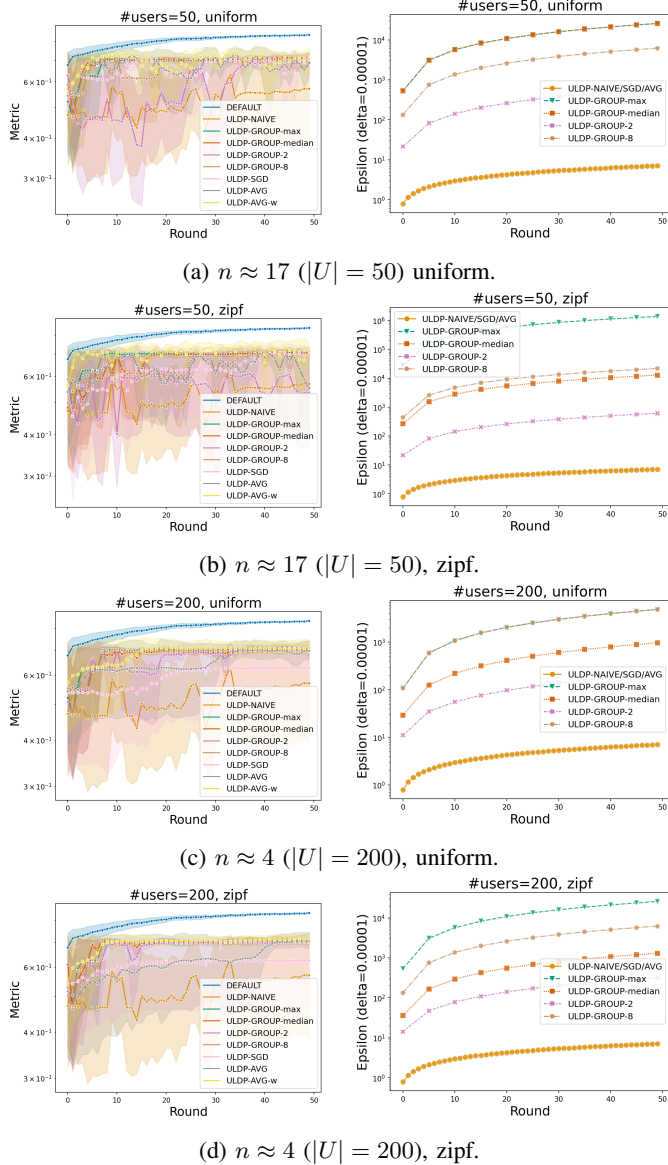


Fig. 10: Privacy-utility trade-offs on TcgaBrca dataset. Test Accuracy (Left), Privacy (Right).

the number of users is large as shown in Figure 11f. This is due to the relatively smaller effect of individual user over fitting caused from non-i.i.d. distribution as the sample size (the number of users) increases.

Figure 12 shows the effect of the better weighting strategy (i.e., ULDP-AVG vs ULDP-AVG-w) on TcgaBrca dataset. Both uniform and zipf have greatly improved in convergence speed with the better weighting strategy. In particular, since the better weighting is adapted to the distribution of the records, it also shows little variance of the results.

**User-level sub-sampling effect.** We evaluate the effect of user-level sub-sampling. The details of the algorithm of ULDP-AVG with user-level sub-sampling is shown in Algorithm 5. The difference from ULDP-AVG highlights in red letters. Figure 13 illustrates that how user-level sub-sampling

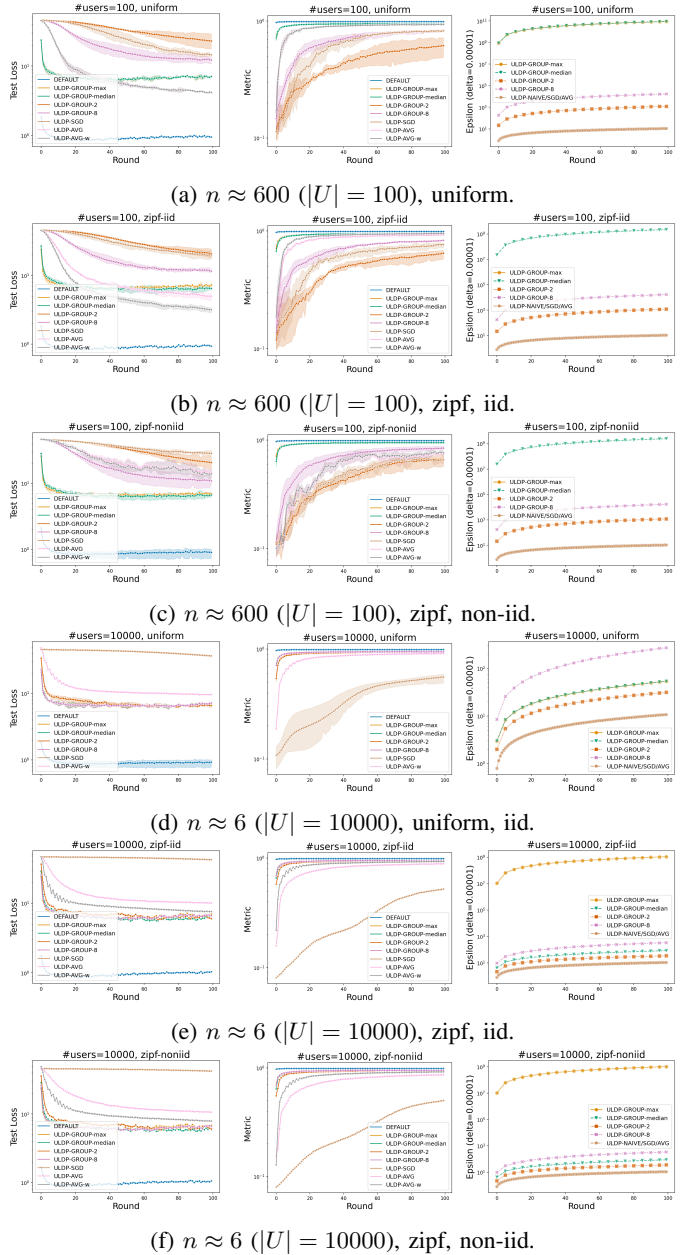


Fig. 11: Privacy-utility trade-offs on MNIST dataset: Test Loss (Left), Accuracy (Middle), Privacy (Right).

affects the privacy-utility trade-offs on Creditcard with 1000 users. We report the test accuracy and ULDP privacy bounds for various sampling rates  $q = 0.1, 0.3, 0.5, 0.7, 1.0$ . Basically, tight privacy bound is obtained at the expense of utility. As the result shows, the degradation of utility due to the sub-sampling could be acceptable to some extent (e.g.,  $q = 0.7$ ) and there could be an optimal point for each setting. Figure 14 illustrates that how user-level sub-sampling affects the privacy-utility trade-offs on MNIST with 10000 users with sampling rates  $q = 0.1, 0.3, 0.5, 1.0$ . The result shows that while privacy is greatly improved, there is less degradation in utility. This is due to the fact that there are a sufficient number of users i.e.,



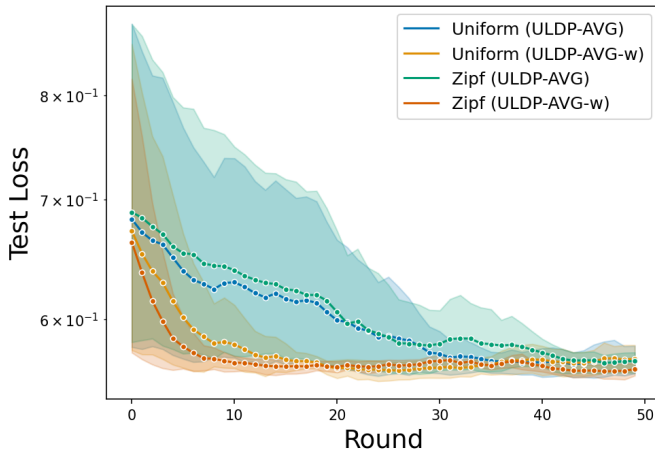
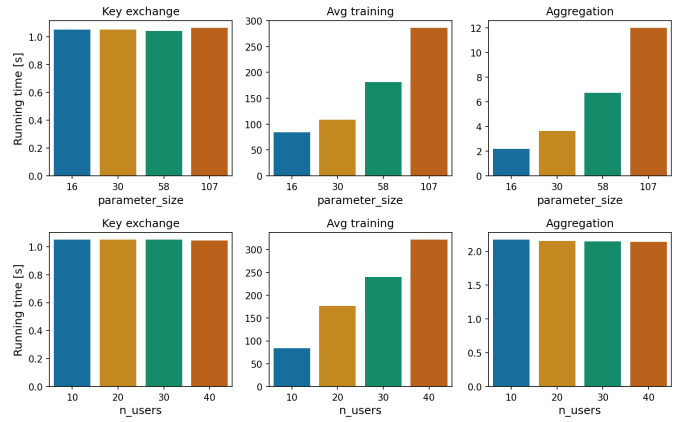


Fig. 12: Test loss of TcgaBrca: the better weighting is effective especially in biased distribution.



d, user-level sub-sampling might

Fig. 15: The dominant execution time of training grows linearly with parameter size and/or the number of users.

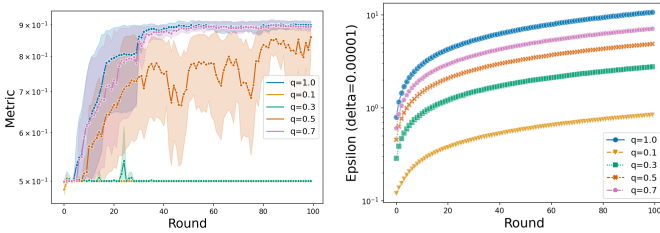


Fig. 13: In Creditcard, user-level sub-sampling achieves a more competitive privacy-utility trade-off.

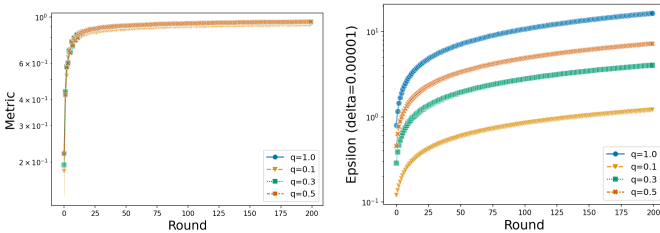


Fig. 14: In MNIST, user-level sub-sampling achieves a more competitive privacy-utility trade-off.

overhead due to the computation with the Paillier encryption, which grows linearly with parameter size and/or the number of users. The larger parameter size increases the aggregation time on the server as well. Our implementation is based on the Python 3.9 library (<https://github.com/data61/python-paillier>) with 3072-bit security, which itself could be made faster by software implementation or hardware accelerators [46]. However, it can be difficult to apply to larger models, such as DNNs, because the execution time increases linearly on a non-negligible scale with parameter size. Therefore, extending the proposed method to deep models with millions of parameters is a future challenge. It may be possible to replace such software-based encryption methods by using hardware-assisted Trusted Execution Environment, which has recently attracted attention in the FL field [47], [48].

10000. In the case of larger users, the effect of sub-sampling is even greater and is likely to become an important technique.

### Overhead of private weighting protocol.

Figure 15 describes the execution times of the proposed private weighting protocol (Protocol 1) with artificial dataset with 10000 samples and model with 16 parameters, 20 users and 3 silos as default. Note that these are on a considerably small scale. The major time-consuming parts of the protocol are key exchange, training in each silo and aggregation on the server. The upper figure shows the execution times on each part of the protocol with various parameter size 16 to 107 and the bottom figure shows the various number of users 10 to 40. The execution time of local training is averaged by silos. The dominant part is the local training part, which is considered to be an

## Proof of Theorem 4

*Proof.* The many of techniques in the following proof are seen in [36], [37], [49].

For convenience, we define following quantities:

$$\begin{aligned} \alpha_t^{s,u} &:= \frac{w_{s,u}C}{\max(C, \eta_l \|\sum_{q \in [Q]} g_{t,q}^{s,u}\|)}, \tilde{\alpha}_t^{s,u} := \frac{w_{s,u}C}{\max(C, \eta_l \|\mathbb{E}[\sum_{q \in [Q]} g_{t,q}^{s,u}]\|)}, \bar{\alpha}_t := \frac{1}{|S||U|} \sum_{s \in S} \sum_{u \in U} \tilde{\alpha}_t^{s,u}, \\ \Delta_t^{s,u} &:= -\eta_l \sum_{q \in [Q]} g_{t,q}^{s,u} \cdot \alpha_t^{s,u}, \tilde{\Delta}_t^{s,u} := -\eta_l \sum_{q \in [Q]} g_{t,q}^{s,u} \cdot \tilde{\alpha}_t^{s,u}, \bar{\Delta}_t^{s,u} := -\eta_l \sum_{q \in [Q]} g_{t,q}^{s,u} \cdot \bar{\alpha}_t, \end{aligned} \quad (6)$$

$$\check{\Delta}_t^{s,u} := -\eta_l \sum_{q \in [Q]} \nabla f_{s,u}(x_{t,q}^{s,u}) \cdot \bar{\alpha}_t, \Delta_t^s := \sum_{u \in U} \Delta_t^{s,u}, \tilde{\Delta}_t^s := \sum_{u \in U} \tilde{\Delta}_t^{s,u}, \bar{\Delta}_t^s := \sum_{u \in U} \bar{\Delta}_t^{s,u}, \check{\Delta}_t^s := \sum_{u \in U} \check{\Delta}_t^{s,u}. \quad (7)$$

where expectation in  $\tilde{\alpha}_t^{s,u}$  is taken over all possible randomness. Due to the smoothness in Assumption 1, we have

$$f(x_{t+1}) \leq f(x_t) + \langle \nabla f(x_t), x_{t+1} - x_t \rangle + \frac{L}{2} \|x_{t+1} - x_t\|^2. \quad (8)$$

The model difference between two consecutive iterations can be represented as

$$x_{t+1} - x_t = \eta_g \frac{1}{|S||U|} \sum_{s \in S} (\Delta_t^s + z_t^s) \quad (9)$$

with random noise  $z_t^s \sim \mathcal{N}(0, I\sigma^2 C^2/|S|)$ . Taking expectation of  $f(x_{t+1})$  over the randomness at communication round  $t$ , we have:

$$\begin{aligned} \mathbb{E}[f(x_{t+1})] &\leq f(x_t) + \langle \nabla f(x_t), \mathbb{E}[x_{t+1} - x_t] \rangle + \frac{L}{2} \mathbb{E}[\|x_{t+1} - x_t\|^2] \\ &= f(x_t) + \eta_g \langle \nabla f(x_t), \mathbb{E} \left[ \frac{1}{|S||U|} \sum_{s \in S} (\Delta_t^s + z_t^s) \right] \rangle + \frac{L}{2} \eta_g^2 \mathbb{E} \left[ \left\| \frac{1}{|S||U|} \sum_{s \in S} (\Delta_t^s + z_t^s) \right\|^2 \right] \\ &= f(x_t) + \eta_g \langle \nabla f(x_t), \mathbb{E} \left[ \frac{1}{|S||U|} \sum_{s \in S} \Delta_t^s \right] \rangle + \frac{L}{2} \eta_g^2 \mathbb{E} \left[ \left\| \frac{1}{|S||U|} \sum_{s \in S} \Delta_t^s \right\|^2 \right] + \frac{L}{2} \eta_g^2 \frac{1}{|S|^2|U|^2} \sigma^2 C^2 d \end{aligned} \quad (10)$$

where  $d$  in the last expression is dimension of  $x_t$  and in the last equation we use the fact that  $z_t^s$  is zero mean normal distribution.

Firstly, we evaluate the first-order term of Eq. (10),

$$\begin{aligned} &\langle \nabla f(x_t), \mathbb{E} \left[ \frac{1}{|S||U|} \sum_{s \in S} \Delta_t^s \right] \rangle \\ &= \langle \nabla f(x_t), \mathbb{E} \left[ \frac{1}{|S||U|} \sum_{s \in S} (\Delta_t^s - \tilde{\Delta}_t^s) \right] \rangle + \langle \nabla f(x_t), \mathbb{E} \left[ \frac{1}{|S||U|} \sum_{s \in S} (\tilde{\Delta}_t^s - \bar{\Delta}_t^s) \right] \rangle + \langle \nabla f(x_t), \mathbb{E} \left[ \frac{1}{|S||U|} \sum_{s \in S} \bar{\Delta}_t^s \right] \rangle, \end{aligned} \quad (11)$$

and the last term of Eq. (11) can be evaluated as follows:

$$\begin{aligned} &\langle \nabla f(x_t), \mathbb{E} \left[ \frac{1}{|S||U|} \sum_{s \in S} \bar{\Delta}_t^s \right] \rangle \\ &= -\frac{\eta_l \bar{\alpha}_t Q}{2} \|\nabla f(x_t)\|^2 - \frac{\eta_l \bar{\alpha}_t}{2Q} \mathbb{E} \left[ \left\| \frac{1}{\eta_l |S||U| \bar{\alpha}_t} \sum_{s \in S} \check{\Delta}_t^s \right\|^2 \right] + \frac{\eta_l \bar{\alpha}_t}{2} \mathbb{E} \left[ \left\| \sqrt{Q} \nabla f(x_t) + \frac{1}{\sqrt{Q} \eta_l |S||U| \bar{\alpha}_t} \sum_{s \in S} \check{\Delta}_t^s \right\|^2 \right]. \end{aligned} \quad (12)$$

This is because  $\mathbb{E} \bar{\Delta}_t^s = \check{\Delta}_t^s$  and  $\langle a, b \rangle = -\frac{1}{2} \|a\|^2 - \frac{1}{2} \|b\|^2 + \frac{1}{2} \|a+b\|^2$  for any vector  $a, b$ .

We further upper bound the last term of Eq. 12 as:

$$\begin{aligned}
\mathbb{E} \left[ \left\| \sqrt{Q} \nabla f(x_t) + \frac{1}{\sqrt{Q} \eta_l |S| |U| \bar{\alpha}_t} \sum_{s \in S} \check{\Delta}_t^s \right\|^2 \right] &= Q \mathbb{E} \left[ \left\| \nabla f(x_t) + \frac{1}{Q \eta_l |S| |U| \bar{\alpha}_t} \sum_{s \in S} \left( \sum_{u \in U} (-\eta_l \sum_{q \in [Q]} \nabla f_{s,u}(x_{t,q}^{s,u}) \cdot \bar{\alpha}_t) \right) \right\|^2 \right] \\
&= Q \mathbb{E} \left[ \left\| \frac{1}{Q |S| |U|} \sum_{s \in S} \sum_{u \in U} \sum_{q \in [Q]} \nabla f_{s,u}(x_t) - \nabla f_{s,u}(x_{t,q}^{s,u}) \right\|^2 \right] \\
&\stackrel{(a1)}{\leq} Q \cdot \frac{1}{Q |S| |U|} \mathbb{E} \left[ \sum_{s \in S} \sum_{u \in U} \sum_{q \in [Q]} \|\nabla f_{s,u}(x_t) - \nabla f_{s,u}(x_{t,q}^{s,u})\|^2 \right] \\
&\stackrel{(a2)}{\leq} \frac{1}{|S| |U|} \sum_{s \in S} \sum_{u \in U} \sum_{q \in [Q]} L^2 \mathbb{E} [\|x_t - x_{t,q}^{s,u}\|^2] \\
&\stackrel{(a3)}{\leq} L^2 5 Q^2 \eta_l^2 (\sigma_l^2 + 6 Q \sigma_g^2) + L^2 30 Q^3 \eta_l^2 \|\nabla f(x_t)\|^2, \tag{13}
\end{aligned}$$

where we use  $\mathbb{E} [\|X_1 + \dots + X_n\|^2] \leq n \mathbb{E} [\|X_1\|^2 + \dots + \|X_n\|^2]$  at (a1), L-smoothness (Assumption 1) at (a2), and Lemma 3 of [49] at (a3).

Secondly, we evaluate the second-order term in Eq. (10) as follows:

$$\begin{aligned}
&\mathbb{E} \left[ \left\| \frac{1}{|S| |U|} \sum_{s \in S} \Delta_t^s \right\|^2 \right] \\
&\leq 3 \mathbb{E} \left[ \left\| \frac{1}{|S| |U|} \sum_{s \in S} \Delta_t^s - \check{\Delta}_t^s \right\|^2 \right] + 3 \mathbb{E} \left[ \left\| \frac{1}{|S| |U|} \sum_{s \in S} \Delta_t^s - \bar{\Delta}_t^s \right\|^2 \right] + 3 \mathbb{E} \left[ \left\| \frac{1}{|S| |U|} \sum_{s \in S} \bar{\Delta}_t^s \right\|^2 \right]. \tag{14}
\end{aligned}$$

This is because  $(a + b + c)^2 \leq 3a^2 + 3b^2 + 3c^2$  holds when  $a = A - B$ ,  $b = B - C$ ,  $c = C$  for all vector  $A, B, C$ . We can bound the expectation in the last term of Eq. (14) as follows:

$$\begin{aligned}
\mathbb{E} \left[ \left\| \frac{1}{|S| |U|} \sum_{s \in S} \bar{\Delta}_t^s \right\|^2 \right] &= \mathbb{E} \left[ \left\| \frac{1}{|S| |U|} \sum_{s \in S} \sum_{u \in U} \left( \eta_l \sum_{q \in [Q]} g_{t,q}^{s,u} \cdot \bar{\alpha}_t \right) \right\|^2 \right] \\
&\stackrel{(a4)}{=} \eta_l^2 \mathbb{E} \left[ \left\| \frac{1}{|S| |U|} \sum_{s \in S} \sum_{u \in U} \sum_{q \in [Q]} \nabla f_{s,u}(x_{t,q}^{s,u}) \cdot \bar{\alpha}_t \right\|^2 + \left\| \frac{1}{|S| |U|} \sum_{s \in S} \sum_{u \in U} \sum_{q \in [Q]} (\nabla f_{s,u}(x_{t,q}^{s,u}) - g_{t,q}^{s,u}) \cdot \bar{\alpha}_t \right\|^2 \right] \\
&= \mathbb{E} \left[ \left\| \frac{1}{|S| |U|} \sum_{s \in S} \check{\Delta}_t^s \right\|^2 \right] + \frac{\eta_l^2 \bar{\alpha}_t^2}{|S|^2 |U|^2} \mathbb{E} \left[ \left\| \sum_{s \in S} \sum_{u \in U} \sum_{q \in [Q]} (\nabla f_{s,u}(x_{t,q}^{s,u}) - g_{t,q}^{s,u}) \right\|^2 \right] \\
&\stackrel{(a5)}{\leq} \mathbb{E} \left[ \left\| \frac{1}{|S| |U|} \sum_{s \in S} \check{\Delta}_t^s \right\|^2 \right] + \frac{\eta_l^2 \bar{\alpha}_t^2}{|S|^2 |U|^2} \mathbb{E} \left[ \sum_{s \in S} \sum_{u \in U} \sum_{q \in [Q]} \|\nabla f_{s,u}(x_{t,q}^{s,u}) - g_{t,q}^{s,u}\|^2 \right] \\
&\leq \mathbb{E} \left[ \left\| \frac{1}{|S| |U|} \sum_{s \in S} \check{\Delta}_t^s \right\|^2 \right] + \frac{\eta_l^2 \bar{\alpha}_t^2}{|S|^2 |U|^2} \sum_{s \in S} \sum_{u \in U} \sum_{q \in [Q]} \sigma_l^2 \\
&\leq \mathbb{E} \left[ \left\| \frac{1}{|S| |U|} \sum_{s \in S} \check{\Delta}_t^s \right\|^2 \right] + \frac{\eta_l^2 \bar{\alpha}_t^2}{|S| |U|} Q \sigma_l^2, \tag{15}
\end{aligned}$$

where we use  $\mathbb{E} [\|X\|^2] = \mathbb{E} [\|X - \mathbb{E}[X]\|^2] + \|\mathbb{E}[X]\|^2$  at (a4), and  $\mathbb{E} [\|X_1 + \dots + X_n\|^2] \leq \mathbb{E} [\|X_1\|^2 + \dots + \|X_n\|^2]$  when  $\forall i, j, i \neq j$ ,  $X_i$  and  $X_j$  are independent and  $\mathbb{E}[X_i] = 0$  and Assumption 2 at (a5).

Lastly, combining all of above, we have

$$\begin{aligned}
\mathbb{E}[f(x_{x+1})] &\leq f(x_t) + \eta_g \langle \nabla f(x_t), \mathbb{E} \left[ \frac{1}{|S||U|} \sum_{s \in S} (\Delta_t^s - \tilde{\Delta}_t^s) \right] \rangle + \eta_g \langle \nabla f(x_t), \mathbb{E} \left[ \frac{1}{|S||U|} \sum_{s \in S} (\check{\Delta}_t^s - \bar{\Delta}_t^s) \right] \rangle \\
&\quad - \frac{1}{2} \eta_g \eta_l \bar{\alpha}_t Q \|\nabla f(x_t)\|^2 - \frac{1}{2} \frac{\eta_g}{Q|S|^2|U|^2 \eta_l \bar{\alpha}_t} \mathbb{E} \left[ \left\| \sum_{s \in S} \check{\Delta}_t^s \right\|^2 \right] \\
&\quad + \frac{\eta_g \eta_l \bar{\alpha}_t}{2} (L^2 5Q^2 \eta_l^2 (\sigma_l^2 + 6Q\sigma_g^2) + L^2 30Q^3 \eta_l^2 \|\nabla f(x_t)\|^2) \\
&\quad + \frac{3}{2} L \eta_g^2 \mathbb{E} \left[ \left\| \frac{1}{|S||U|} \sum_{s \in S} \Delta_t^s - \tilde{\Delta}_t^s \right\|^2 \right] + \frac{3}{2} L \eta_g^2 \mathbb{E} \left[ \left\| \frac{1}{|S||U|} \sum_{s \in S} \tilde{\Delta}_t^s - \bar{\Delta}_t^s \right\|^2 \right] + \frac{3}{2} L \eta_g^2 \frac{1}{|S|^2|U|^2} \mathbb{E} \left[ \left\| \sum_{s \in S} \check{\Delta}_t^s \right\|^2 \right] \\
&\quad + \frac{3}{2} \frac{\eta_g^2 \eta_l^2 \bar{\alpha}_t^2 L Q \sigma_l^2}{|S||U|} + \frac{1}{2} \frac{L \eta_g^2 \sigma^2 C^2 d}{|S|^2|U|^2} \\
&= f(x_t) - \left( \frac{1}{2} \eta_l \eta_g \bar{\alpha}_t Q - \frac{\eta_g \eta_l \bar{\alpha}_t}{2} L^2 30Q^3 \eta_l^2 \right) \|\nabla f(x_t)\|^2 \\
&\quad - \left( \frac{1}{2} \frac{\eta_g}{Q|S|^2|U|^2 \eta_l \bar{\alpha}_t} - \frac{3}{2} L \eta_g^2 \frac{1}{|S|^2|U|^2} \right) \mathbb{E} \left[ \left\| \sum_{s \in S} \check{\Delta}_t^s \right\|^2 \right] \\
&\quad + \frac{\eta_g \eta_l \bar{\alpha}_t}{2} L^2 5Q^2 \eta_l^2 (\sigma_l^2 + 6Q\sigma_g^2) + \frac{3}{2} \frac{\eta_g^2 \eta_l^2 \bar{\alpha}_t^2 L Q \sigma_l^2}{|S||U|} + \frac{1}{2} \frac{L \eta_g^2 \sigma^2 C^2 d}{|S|^2|U|^2} \\
&\quad + \underbrace{\eta_g \langle \nabla f(x_t), \mathbb{E} \left[ \frac{1}{|S||U|} \sum_{s \in S} (\Delta_t^s - \tilde{\Delta}_t^s) \right] \rangle + \eta_g \langle \nabla f(x_t), \mathbb{E} \left[ \frac{1}{|S||U|} \sum_{s \in S} (\check{\Delta}_t^s - \bar{\Delta}_t^s) \right] \rangle}_{A_1} \\
&\quad + \underbrace{\frac{3}{2} L \eta_g^2 \mathbb{E} \left[ \left\| \frac{1}{|S||U|} \sum_{s \in S} \Delta_t^s - \tilde{\Delta}_t^s \right\|^2 \right] + \frac{3}{2} L \eta_g^2 \mathbb{E} \left[ \left\| \frac{1}{|S||U|} \sum_{s \in S} \tilde{\Delta}_t^s - \bar{\Delta}_t^s \right\|^2 \right]}_{A_2} \\
&\stackrel{(a6)}{\leq} f(x_t) - \eta_l \eta_g \bar{\alpha}_t Q \left( \frac{1}{2} - 15L^2 Q^2 \eta_l^2 \right) \|\nabla f(x_t)\|^2 \\
&\quad + \frac{\eta_g \eta_l \bar{\alpha}_t}{2} L^2 5Q^2 \eta_l^2 (\sigma_l^2 + 6Q\sigma_g^2) + \frac{3}{2} \frac{\eta_g^2 \eta_l^2 \bar{\alpha}_t^2 L Q \sigma_l^2}{|S||U|} + \frac{1}{2} \frac{L \eta_g^2 \sigma^2 C^2 d}{|S|^2|U|^2} + A_1 + A_2 \\
&\stackrel{(a7)}{\leq} f(x_t) - c \eta_l \eta_g \bar{\alpha}_t Q \|\nabla f(x_t)\|^2 + \frac{\eta_g \eta_l \bar{\alpha}_t}{2} L^2 5Q^2 \eta_l^2 (\sigma_l^2 + 6Q\sigma_g^2) + \frac{3}{2} \frac{\eta_g^2 \eta_l^2 \bar{\alpha}_t^2 L Q \sigma_l^2}{|S||U|} + \frac{1}{2} \frac{L \eta_g^2 \sigma^2 C^2 d}{|S|^2|U|^2} + A_1 + A_2
\end{aligned} \tag{16}$$

where (a6) follows from  $\left( \frac{1}{2} \frac{\eta_g}{Q|S|^2|U|^2 \eta_l \bar{\alpha}_t} - \frac{3}{2} L \eta_g^2 \frac{1}{|S|^2|U|^2} \right) \geq 0$  if  $\eta_g \eta_l \leq \frac{1}{3QL\bar{\alpha}_t}$  and replacing the last terms with  $A_1$  and  $A_2$ , and (a7) holds because there exists a constant  $c > 0$  satisfying  $\left( \frac{1}{2} - 15L^2 Q^2 \eta_l^2 \right) > c > 0$  if  $\eta_l < \frac{1}{\sqrt{30QL}}$ . Divide both sides

of (16) by  $c\eta_l\eta_gQ\bar{\alpha}_t$ , sum over  $t$  from 0 to  $T-1$ , divide both sides by  $T$ , and rearrange, we have

$$\begin{aligned}
\frac{1}{T} \sum_{t=0}^{T-1} \mathbb{E} \left[ \|\nabla f(x_t)\|^2 \right] &\leq \frac{1}{cT\eta_g\eta_lQ} \left( \mathbb{E} \left[ \frac{f(x_0)}{\bar{\alpha}_0} \right] - \mathbb{E} \left[ \frac{f(x_T)}{\bar{\alpha}_{T-1}} \right] \right) \\
&+ \frac{5}{2c} L^2 Q \eta_l^2 (\sigma_l^2 + 6Q\sigma_g^2) + \frac{3L\eta_g\eta_l\sigma_l^2}{2c|S||U|} \frac{1}{T} \sum_{t=0}^{T-1} \bar{\alpha}_t + \frac{L\eta_g\sigma^2 C^2 d}{2c\eta_l Q|S|^2|U|^2} \frac{1}{T} \sum_{t=0}^{T-1} \frac{1}{\bar{\alpha}_t} \\
&+ \underbrace{\frac{1}{c\eta_l Q T} \sum_{t=0}^{T-1} \frac{1}{\bar{\alpha}_t} \mathbb{E} \left[ \langle \nabla f(x_t), \mathbb{E} \left[ \frac{1}{|S||U|} \sum_{s \in S} (\Delta_t^s - \tilde{\Delta}_t^s) \right] \rangle + \langle \nabla f(x_t), \mathbb{E} \left[ \frac{1}{|S||U|} \sum_{s \in S} (\tilde{\Delta}_t^s - \bar{\Delta}_t^s) \right] \rangle \right]}_{B_1} \\
&+ \underbrace{\frac{3L\eta_g}{2c\eta_l Q T} \sum_{t=0}^{T-1} \frac{1}{\bar{\alpha}_t} \left( \mathbb{E} \left[ \left\| \frac{1}{|S||U|} \sum_{s \in S} \Delta_t^s - \tilde{\Delta}_t^s \right\|^2 \right] + \mathbb{E} \left[ \left\| \frac{1}{|S||U|} \sum_{s \in S} \tilde{\Delta}_t^s - \bar{\Delta}_t^s \right\|^2 \right] \right)}_{B_2}. \tag{17}
\end{aligned}$$

Let  $\max_{s \in S, u \in U, t \in [T]} \left( \frac{C}{\max(C, \eta_l \mathbb{E}[\sum_{q \in [Q]} g_{t,q}^{s,u}])} \right)$  be  $\bar{C}$ , and  $\min_{s \in S, u \in U, t \in [T]} \left( \frac{C}{\max(C, \eta_l \mathbb{E}[\sum_{q \in [Q]} g_{t,q}^{s,u}])} \right)$  be  $\underline{C}$ ,  $\frac{1}{|S|}\underline{C} \leq \bar{\alpha}_t \leq \frac{1}{|S|}\bar{C}$  since  $\bar{\alpha}_t$ 's definition and  $\frac{1}{|S|} \sum_{s \in S} w_{s,u} = \frac{1}{|S|}$ . Using this, (17) is evaluated as follows:

$$\begin{aligned}
\frac{1}{T} \sum_{t=0}^{T-1} \mathbb{E} \left[ \|\nabla f(x_t)\|^2 \right] &\leq \frac{1}{cT\eta_g\eta_lQ|S|} \left( \mathbb{E} \left[ \frac{f(x_0)}{\underline{C}} \right] - \mathbb{E} \left[ \frac{f(x_T)}{\bar{C}} \right] \right) \\
&+ \frac{5}{2c} L^2 Q \eta_l^2 (\sigma_l^2 + 6Q\sigma_g^2) + \frac{3\bar{C}L\eta_g\eta_l\sigma_l^2}{2c|S|^2|U|} + \frac{L\eta_g\sigma^2 C^2 d}{2c\underline{C}\eta_l Q|S||U|^2} \\
&+ \underbrace{\frac{|S|}{c\underline{C}\eta_l Q T} \sum_{t=0}^{T-1} \mathbb{E} \left[ \langle \nabla f(x_t), \mathbb{E} \left[ \frac{1}{|S||U|} \sum_{s \in S} (\Delta_t^s - \tilde{\Delta}_t^s) \right] \rangle + \langle \nabla f(x_t), \mathbb{E} \left[ \frac{1}{|S||U|} \sum_{s \in S} (\tilde{\Delta}_t^s - \bar{\Delta}_t^s) \right] \rangle \right]}_{B_1} \\
&+ \underbrace{\frac{3L\eta_g|S|}{2c\underline{C}\eta_l Q T} \sum_{t=0}^{T-1} \left( \mathbb{E} \left[ \left\| \frac{1}{|S||U|} \sum_{s \in S} \Delta_t^s - \tilde{\Delta}_t^s \right\|^2 \right] + \mathbb{E} \left[ \left\| \frac{1}{|S||U|} \sum_{s \in S} \tilde{\Delta}_t^s - \bar{\Delta}_t^s \right\|^2 \right] \right)}_{B_2}. \tag{18}
\end{aligned}$$

$B_1$  and  $B_2$  is upper-bounded as follows:

$$\begin{aligned}
B_1 &\leq \frac{|S|}{c\underline{C}\eta_l Q T} \sum_{t=0}^{T-1} \mathbb{E} \left[ \langle \nabla f(x_t), \mathbb{E} \left[ \frac{1}{|S||U|} \sum_{s \in S} \sum_{u \in U} |\Delta_t^{s,u} - \tilde{\Delta}_t^{s,u}| \right] \rangle + \langle \nabla f(x_t), \mathbb{E} \left[ \frac{1}{|S||U|} \sum_{s \in S} \sum_{u \in U} |\tilde{\Delta}_t^{s,u} - \bar{\Delta}_t^{s,u}| \right] \rangle \right] \\
&\leq \frac{G^2}{c\underline{C}|U|T} \sum_{t=0}^{T-1} \mathbb{E} \left[ \sum_{s \in S} \sum_{u \in U} (|\alpha_t^{s,u} - \tilde{\alpha}_t^{s,u}| + |\tilde{\alpha}_t^{s,u} - \bar{\alpha}_t|) \right], \\
B_2 &\stackrel{(a8)}{\leq} \frac{3L\eta_g|S|}{2c\underline{C}\eta_l Q T} \sum_{t=0}^{T-1} \left( \mathbb{E} \left[ \frac{1}{|S||U|} \sum_{s \in S} \sum_{u \in U} |\Delta_t^{s,u} - \tilde{\Delta}_t^{s,u}|^2 \right] + \mathbb{E} \left[ \frac{1}{|S||U|} \sum_{s \in S} \sum_{u \in U} |\tilde{\Delta}_t^{s,u} - \bar{\Delta}_t^{s,u}|^2 \right] \right) \\
&\leq \frac{3L\eta_g\eta_l Q G^2}{2c\underline{C}|U|T} \sum_{t=0}^{T-1} \mathbb{E} \left[ \sum_{s \in S} \sum_{u \in U} (|\alpha_t^{s,u} - \tilde{\alpha}_t^{s,u}|^2 + |\tilde{\alpha}_t^{s,u} - \bar{\alpha}_t|^2) \right] \tag{19}
\end{aligned}$$

with

$$\begin{aligned}
|\Delta_t^{s,u} - \tilde{\Delta}_t^{s,u}| &\leq \eta_l Q G |\alpha_t^{s,u} - \tilde{\alpha}_t^{s,u}|, \\
|\tilde{\Delta}_t^{s,u} - \bar{\Delta}_t^{s,u}| &\leq \eta_l Q G |\tilde{\alpha}_t^{s,u} - \bar{\alpha}_t|, \tag{20}
\end{aligned}$$

by Assumption 3 of globally bounded gradients, and we use the same technique at (a8) as (a1).  $\square$